AFRL-IF-RS-TR-2002-93
Final Technical Report
May 2002

PINPOINT PHASE 1

BAE Systems

APPROVED FOR PUBLIC RELEASE; DISTRIBUTION UNLIMITED.

AIR FORCE RESEARCH LABORATORY
INFORMATION DIRECTORATE
ROME RESEARCH SITE
ROME, NEW YORK

This report has been reviewed by the Air Force Research Laboratory, Information Directorate, Public Affairs Office (IFOIPA) and is releasable to the National Technical Information Service (NTIS). At NTIS it will be releasable to the general public, including foreign nations.

AFRL-IF-RS-TR-2002-93 has been reviewed and is approved for publication.

APPROVED: 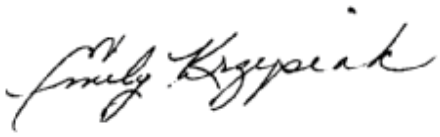

EMILY A. KRZYSIAK
Project Engineer

FOR THE DIRECTOR: 

JOSEPH CAMERA, Chief
Information & Intelligence Exploitation Division
Information Directorate

REPORT DOCUMENTATION PAGE

Form Approved
OMB No. 074-0188

1. AGENCY USE ONLY (Leave blank)	2. REPORT DATE	3. REPORT TYPE AND DATES COVERED
	MAY 2002	Final Sep 00 – Jan 02

4. TITLE AND SUBTITLE
PINPOINT PHASE 1

5. FUNDING NUMBERS
C - F30602-99-D-0152/0005
PE - N/A
PR - 1027
TA - QA
WU - 05

6. AUTHOR(S)
C. R. Clark and R. E. Shanafelt

7. PERFORMING ORGANIZATION NAME(S) AND ADDRESS(ES)
Prime: BAE Systems
111 East Chestnut Street
Rome New York 13440

Sub: Radix Technologies, Incorporated
329 North Bernardo Avenue
Mountain View California 94043

8. PERFORMING ORGANIZATION REPORT NUMBER
N/A

9. SPONSORING / MONITORING AGENCY NAME(S) AND ADDRESS(ES)
Air Force Research Laboratory/IFEC
32 Brooks Road
Rome New York 13441-4114

10. SPONSORING / MONITORING AGENCY REPORT NUMBER
AFRL-IF-RS-TR-2002-93

11. SUPPLEMENTARY NOTES
AFRL Project Engineer: Emily A. Krzysiak/IFEC/(315) 330-7151/Emily.Krzysiak@rl.af.mil

12a. DISTRIBUTION / AVAILABILITY STATEMENT
APPROVED FOR PUBLIC RELEASE; DISTRIBUTION UNLIMITED.

12b. DISTRIBUTION CODE

13. ABSTRACT ***(Maximum 200 Words)***
The purpose of the PinPoint program is to integrate adaptive beamforming techniques for co-channel interference cancellation, with Time Difference of Arrival - Differential Doppler (TDOA-DD)processing for rapid and precise Geolocation of tactical emitters in a dense co-channel signal and interference environment. The PinPoint program is intended to complement the existing CHAALS system by providing advanced techniques that address the Army's longer-term Objective System requirements.

The end goal of the PinPoint multi-phase program is to integrate PinPoint precision geolocation capability with a co-channel signal intercept system employing multiple multi-antenna airborne collection platforms, such as ACS, to provide a complete, precise and real-time geographical image of the modem battlefield signals environment. The co-channel interference look-through capability provided by PinPoint and related co-channel detect, DF, and beamforming copy front-end assets will enable the battlefield environment to be accurately monitored deep behind the forward troops from airborne platforms positioned at safe standoff distances.

14. SUBJECT TERMS
Precision Geolocation, Adaptive Beamforming, Interference Cancellation, TDOA, Differential Doppler, Battlefield mapping

15. NUMBER OF PAGES
72

16. PRICE CODE

17. SECURITY CLASSIFICATION OF REPORT	18. SECURITY CLASSIFICATION OF THIS PAGE	19. SECURITY CLASSIFICATION OF ABSTRACT	20. LIMITATION OF ABSTRACT
UNCLASSIFIED	UNCLASSIFIED	UNCLASSIFIED	UL

Table of Contents

Table of Figures

Table of Tables

Executive Summary

The purpose of the PinPoint program is to integrate adaptive beamforming techniques for co-channel interference cancellation, with Time Difference of Arrival – Differential Doppler (TDOA-DD) processing for rapid and precise geolocation of tactical emitters in a dense co-channel signal and interference environment. The PinPoint program is intended to complement the existing CHAALS system by providing advanced techniques that address the Army's longer term Objective System requirements.

The end goal of the PinPoint multi-phase program is to integrate PinPoint precision geolocation capability with a co-channel signal intercept system employing multiple multi-antenna airborne collection platforms, such as ACS, to provide a complete, precise and real-time geographical image of the modern battlefield signals environment. The co-channel interference look-through capability provided by PinPoint and related co-channel detect, DF, and beamforming copy front-end assets will enable the battlefield environment to be accurately monitored deep behind the forward troops from airborne platforms positioned at safe standoff distances.

Simulation results indicate that modern, low-power single-channel tactical emitters (conventional and LPI) operating in closely spaced nets underneath broadcast TV interference will be reliably detected and precisely geolocated, meeting or exceeding the ACS-ORD Target Development and Acquisition specifications at ranges of 200-250 km, with detection-cued collect durations on the order of two seconds in the VHF band. In general, the co-channel interference mitigation techniques employed by PinPoint yield detection and geolocation performance in dense co-channel environments such as the VHF and UHF Broadcast TV bands that is similar to performance levels attained by conventional systems in clear (interference-free) bands. In addition, even in interference-free conditions, the PinPoint approach enhances both detection and geolocation accuracy for low-power, low duty-cycle signals through coherent beamforming gain.

The Phase 1 program, reported on herein, was refocused from the original plan to support a more incremental, staggered approach to system development and flight testing than had been planned during the Phase 0 study, in order to support early flight testing in Phase 2. The PinPoint program will also be merged with the ongoing, multi-phase NRC signal classification program during Phase 2 to demonstrate end-to-end real-time co-channel detect, classify and and geolocate capability against conventional tactical signals. Flight testing of similar capabilities against LPI tactical signals is planned for Phase 3.

The combination of PinPoint and NRC technologies will yield a dramatic improvement in battlefield mapping capability beyond that of currently fielded systems. The system detection and copy footprint is greatly increased, enabling standoff coverage of the entire battlespace for even low-power handheld emitters with a high probability of intercept even in dense interference environments. As a result, accurate classification and precision geolocation is obtained on individual emissions for a comprehensive and real-time situational awareness and battlefield mapping capability, which in turn enables greatly enhanced emitter tracking and network analysis capabilities.

1. Introduction

The purpose of the PinPoint program is to integrate adaptive beamforming techniques for co-channel interference cancellation, with Time Difference of Arrival – Differential Doppler (TDOA-DD) processing for rapid and precise geolocation of tactical emitters in a dense co-channel signal and interference environment. The PinPoint program is intended to complement the existing CHAALS system by providing advanced techniques that address the Army's longer term Objective System requirements.

Interference cancellation improves SIGINT performance on several fronts. The signal detection range is greatly increased, and the signal is copied from multiple platforms independently with high fidelity, which substantially reduces the TDOA-DD signal processing complexity and data link bandwidths. The short collect times reduce complexity, latency, and link bandwidth, and also simplify the motion compensation approach. Geolocation tasking is simplified as well, and it becomes very feasible to obtain a precision geolocation on each signal-up. As a result, geolocation can be used to assist the downstream processes, such as report association, tracking, and net formation.

The PinPoint program is structured as a multi-phase effort, which began with the Phase 0 feasibility study that was completed in Q4, 2000. The Phase 0 study identified and addressed the critical-technology risk areas associated with integrating adaptive beamforming with precision geolocation through a combination of analysis, algorithm development, simulation, and architecture trades. Phase 0 focused primarily on precision geolocation of VHF single-channel tactical conventional and LPI emitters in a broadcast TV environment.

The Phase 1 program began at the end of Phase 0 and extended into Q4, 2001. Phase 1 entailed detailed algorithm development and risk reduction efforts via Matlab simulation, and culminated in the development of a simulated-data driven geolocation system for conventional signals, with geolocation map display, ready for integration into multi-antenna collection and signal processing assets for flight testing under the Phase 2 program.

The results of the Phase 1 effort, reported on herein, include:

- Development, refinement and testing of coarse geolocation cueing and motion compensated fine geolocation algorithms for LPI geolocation, using a simple platform turbulence model;
- Development of a map display capability that supports all currently anticipated flight testing and demonstration requirements of the Pinpoint program through the early flight test phases;
- Development of a data simulator for multi-antenna airborne collection platforms with AM/FM Voice and FSK data nets operating in Broadcast TV and LPI interference;
- A hardware and software PinPoint conventional-signal co-channel geolocation system that operates with simulated data, and will be migrated in Phase 2 for early flight testing; and
- Detailed recommendations for Phase 2 hardware and system design and flight testing that support further developments in Phase 3 and beyond.

The original Phase 1 effort was structured under the presumption that Phase 2 would utilize PinPoint-compatible front-end SIGINT functions from LBSS, via the Army Test Unit. These functions would have included the following:

- Signal search, detect, DF and pre-D data collection functions, with full operator control of reporting and automatic tasking through general and directed search lists
- Complete LPI signal processing, including detection, tracking and pre-D data collection
- Receiver TDOA compensation tasking
- Precision navigation, timing and ultrastable frequency reference through GPS-INS and a Rb standard

Because of the desire for a rapid deployment of flight-testable equipment for Phase 2, the presumptions made at the beginning of Phase 1 are no longer valid. The program was therefore replanned in order to adequately address the new PinPoint program requirements efficiently under the Phase 1 effort, in close coordination with other programs with the Army.

The program focus shifted to development and implementation of the key algorithms required to demonstrate beamformed multi-sensor TDOA-DD processing for conventional emitters. These key algorithms include the following:

- Co-channel signal detection to cue the data collection, beamforming and geolocation processing
- Adaptive spatial beamforming for cochannel interference mitigation and beamformer gain SNR enhancement
- Precision emitter location estimation using correlation ambiguity function (CAF) processing
- Implementation of map displays using off-the-shelf mapping functions and tools

In addition, a multi-channel, multi-platform data simulation was developed that can generate several minutes of narrowband data with various interference sources and temporally overlapping traffic from multiple tactical single-channel conventional nets, with dynamic platform motion effects including turbulence and turns.

The LPI algorithm development results are reported on in Section 2. The conventional algorithms and their implementational forms for Phase 1 and Phase 2 are discussed in Section 3. The Phase 1 Demonstration System hardware configuration, HMI/display software and simulated geolocation results for conventional signals are presented in Section 4. Details of the current multi-phase program migration plan are given in Section 5. The conclusions and summarized recommendations are given in Section 6, and the military signifigance of the PinPoint Multi-Phase Program is discussed in Section 7.

2. LPI Algorithm Refinements and Simulation Results

The precision geolocation algorithm for LPI emitters has been implemented in MatLab and tested under various dynamic platform effects via functional simulation. At this point, we have a high degree of confidence in the efficacy of the LPI precision geolocation approach and strongly recommend that the LPI effort be continued under Phase 2, for eventual real-time implementation and flight testing under Phase 3.

The results of the Phase 1 simulation and modeling efforts are given in the following sections. In particular, these results address the coarse geolocation algorithms used for initial location cuing, platform motion modeling, motion compensation, and precision geolocation of LPI emitters.

2.1 LOB Triangulation and Coarse Geolocation.

The geolocation transformation (conversion of TDOA and FDOA measurements to target location) is implemented iteratively based on the calculated TDOA and FDOA gradient functions, using the Modified Gauss-Newton (MGN) method. The MGN approach is highly flexible and efficiently supports fusion of any combination of TDOA, FDOA, and LOB measurements from any number of platforms.

The MGN method does require initial location cueing however, and can converge to ambiguous local minima of the error function when the initial cueing error is large. The cueing problem is resolved by LOB triangulation if DF information is available. Otherwise, as is anticipated in the PinPoint Phase 2 field tests, the iteration can be repeated over a coarse grid of cue points covering the area of interest in which case the result with lowest residual error is selected as the final answer.

In general, the two-platform TDOA-FDOA geolocation solution is ambiguous over parts of the coverage area, as illustrated in Figure 2-1. In these cases, DF is needed to resolve the ambiguity.

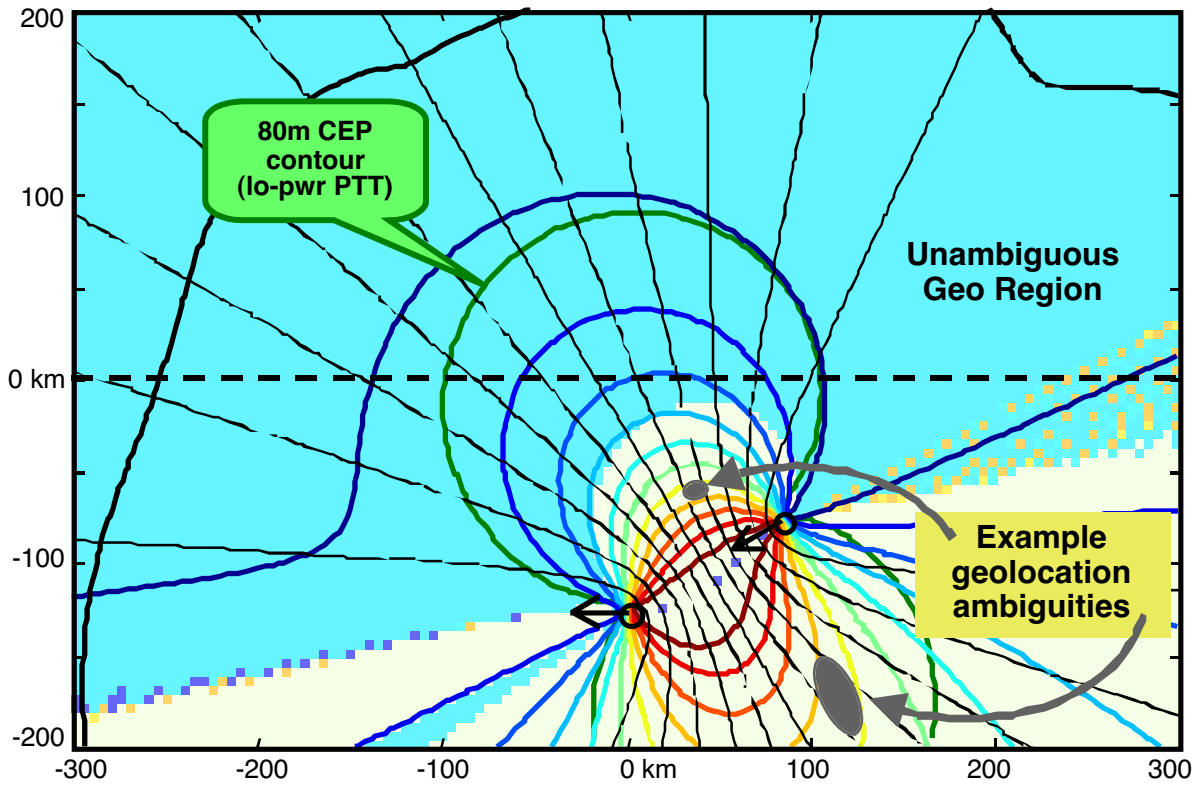

Figure 2-1. Two-Platform TDOA-FDOA Geolocation Ambiguities.

As an alternative to full-area coarse-grid cueing, we can restrict the cue points to lie along the TDOA hyperbola in the plane tangent to the earth's surface at a reference latitude-longitude-altitude, e.g. in the center of the area of interest or at the ground-station location. In fact, the FDOA along that hyperbola can be computed to determine the limiting and local extremal values, to determine precisely how many ambiguities exist and their locations, on the reference plane. For coarse geolocations and over geometries commensurate with tactical Corps Echelon operations, these planar locations are sufficiently accurate to determine lat-long and/or to cue the fine-CAF precision geolocation processing.

The accuracies of the various combinations of LOB, TDOA, and FDOA coarse-geolocation are shown in Figure 2-2, in terms of the 95% error ellipse for each geolocation mode based on the component measurement SINR errors. The platform baseline is 180 km, and the target location is 250 km north and 100 km east of the baseline center. The signal strength is 12 and 15 dB at platforms 1 and 2 respectively, and has a bandwidth of 20 kHz at a carrier frequency of 60 MHz. The collect duration is 200 mSec, and the LOB accuracy at each platform is 0.5 degrees RMS.

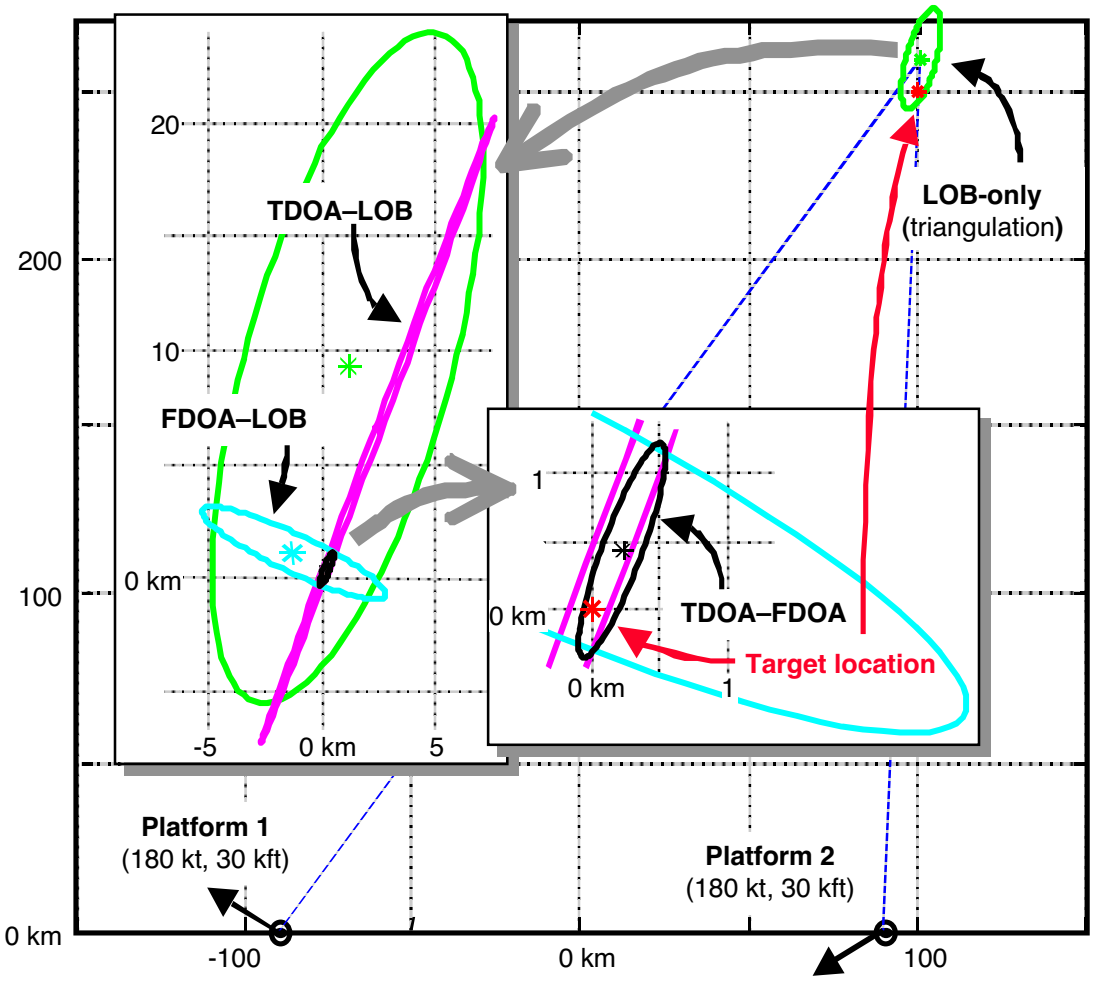

Figure 2-2. LOB-Triangulation and Coarse Geolocation 95% Error Ellipses.

This selection of input parameters yields representative accuracies for LOB and TDOA for low-power tactical LPI coarse-geolocation, and representative TDOA and FDOA accuracies for short collects of conventional signals as might be acquired in operational systems through extended dwell tasking. The FDOA accuracies are also representative of LPI coarse-geolocation measurements at UHF.

Two-platform LOB triangulation is performed in the reference plane tangent to the earth at a selected reference origin (latitude-longitude). For this calculation, it suffices to correct the LOB from each platform for local North (the North direction projected onto the reference plane), compute the linear intersection point, and correct the z-component for spherical-earth rolloff relative to the origin.

Two-platform TDOA yields what amounts to an extremely precise LOB measurement at this range. The LOB data then serves to give coarse range limits on the TDOA-only measurement. This location mode is relevant for coarse geolocation of very short-duration signals such as radar pulses, and can be very useful for geolocation-assisted pulse association.

Two-platform FDOA in this scenario is nearly orthogonal to TDOA. Especially with conventional FM Voice, the first few hundred mSec of the transmission may be unmodulated and early collections may yield only FDOA results. Otherwise, the combination of TDOA and FDOA yields a small, accurate TDOA-FDOA error ellipse. The TDOA-FDOA location can then be combined with the LOB-triangulation result, but generally the resulting error ellipse is virtually unchanged since the LOB error is so much larger than the TDOA-FDOA error. However, a consistency check can reveal FDOA errors due to target motion, for vehicular emitters.

The error ellipse dimensions are tabulated in Table 2-1 for each of the geolocation cases shown in Figure 2-2. Note that these TDOA and FDOA results do not contain navigation, timing or reference oscillator errors, but these errors are expected to be kept small relative to the receiver noise (SINR) error component for coarse geolocation.

Table 2-1. Coarse Geolocation at 60 MHz, Example Results (95% Error Ellipse)

Geo Algorithm	**95% Error Ellipse Axes**		**Miss Distance** (example case)	**Probability of Fit** (fixed target test)
	Major (+/-)	Minor (+/-)		
LOB Triangulate	15.2 km	4.5 km	9.3 km	–
LOB + TDOA	14.6 km	150 m	7.0 km	0.26
LOB + FDOA	4.4 km	840 m	1.7 km	0.19
TDOA-FDOA	840 m	150 m	490 m	–
TDOA-FDOA-LOB	840 m	150 m	510 m	0.28

The LOB fusion cases are overdetermined in that two-dimensional location (latitude-longitude) is computed from three or four independent measurements. As a result, they yield nonzero residual modeling errors, which are expected to follow a chi-squared distribution with respectively 1, 1, and 2 degrees of freedom for the two-platform LOB-TDOA, LOB-FDOA, and LOB-TDOA-FDOA cases. The P-score for this statistic in the illustrated case is given in the last column of Table 2-1. For LOB-TDOA, a low P-score might indicate either a wild bearing or faulty TDOA measurement. For the FDOA cases, low P-scores can be interpreted as indicative of moving targets. However, a slowly moving target such as a handheld emitter would still yield a moderate P-score (reasonable model fit) as long as the resulting location solution is still within the LOB-only error ellipse.

2.2 Platform Motion Modeling.

Platform motion is modeled as a level (constant-altitude) flight path with fixed turn rate (zero, for nominally straight flight) with an additive band-limited gaussian process in acceleration to model turbulence. The platform roll angle is calculated based on the turn rate. The Conventional Signal Simulator, currently under development, allows variations in turn rate and linearly ramps the roll angle over a defined time interval when the turn rate changes. Platform attitude angles are not affected by turbulence accelerations in this simulation.

The turbulence model is currently isotropic; the acceleration processes are independent and identically distributed in each of the three coordinate axes. Therefore, the coordinate reference frame is irrelevant to the model, and we can use the same process in either platform-local or geocentric coordinates. More detailed models might be nonisotropic and therefore would require more attention be paid to the coordinate transformations, perhaps even based on platform attitude.

The turbulence intensity is specified as an rms acceleration per axis in g's, typically 0.1 g. The band-limited filter response is shown in Figure 2-3, and consists of two first-order rolloffs, one at 1 Hz and another at 5 Hz.

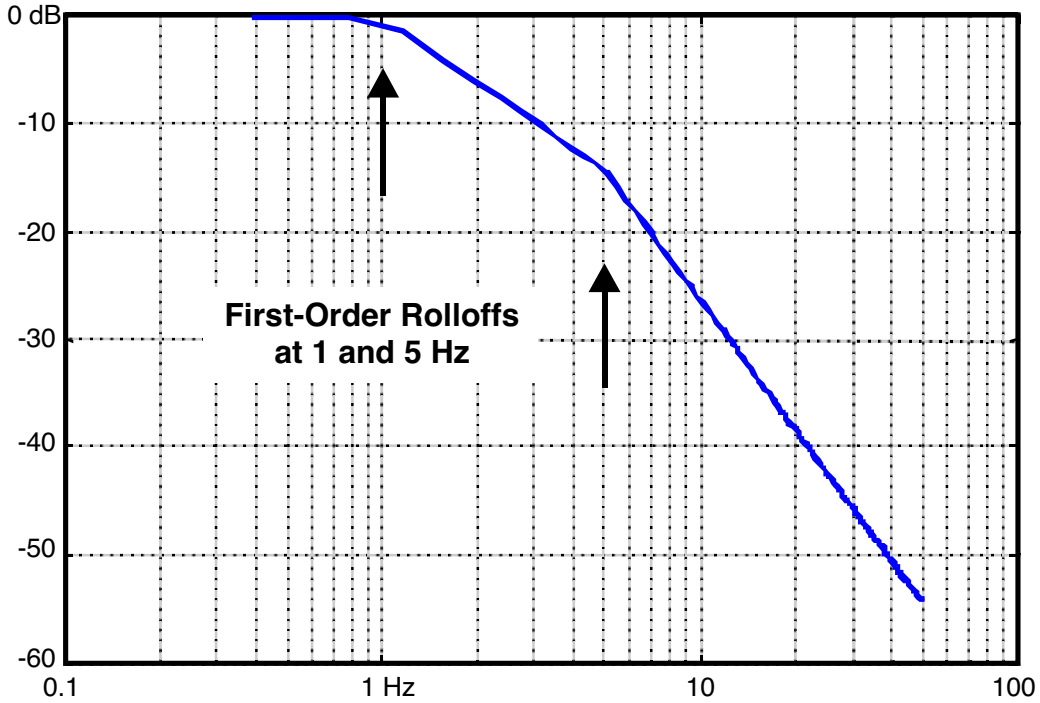

Figure 2-3. Platform Turbulence Model Lowpass Response.

The acceleration profiles for a two-second run are shown in Figure 2-4 for each coordinate axis of two platforms, both undergoing 0.1 g rms turbulence per axis in otherwise straight and level flight.

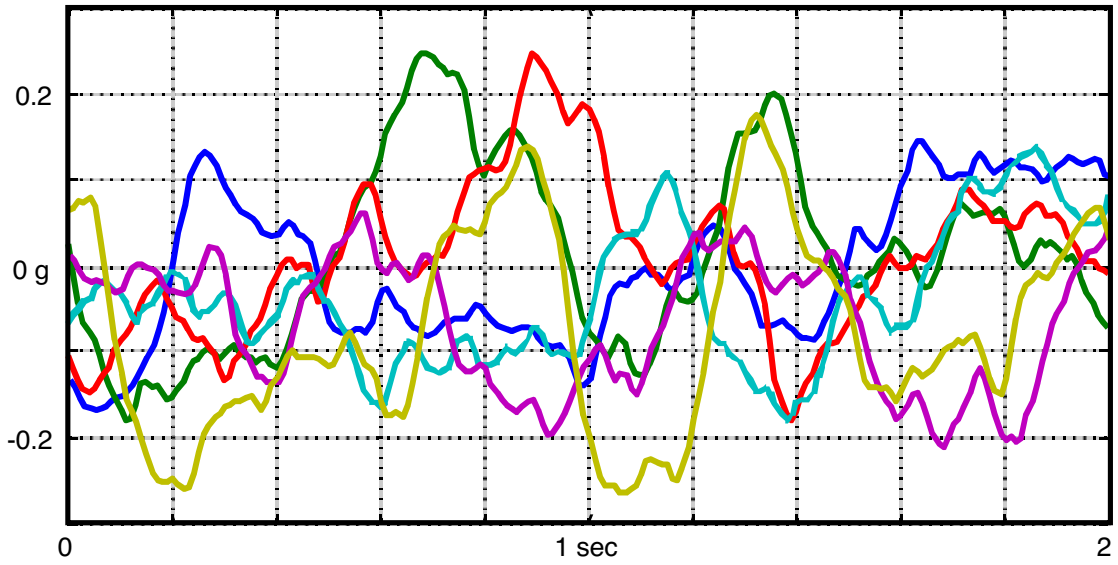

Figure 2-4. Turbulence Accelerations, Each Coordinate (Two Platforms).

The altitudes of the platforms' flight paths are shown in Figure 2-5. The flight paths vary from nominal altitude over a range of about 30 cm during two seconds. Similar variations from the nominal flight path are seen in the horizontal plane.

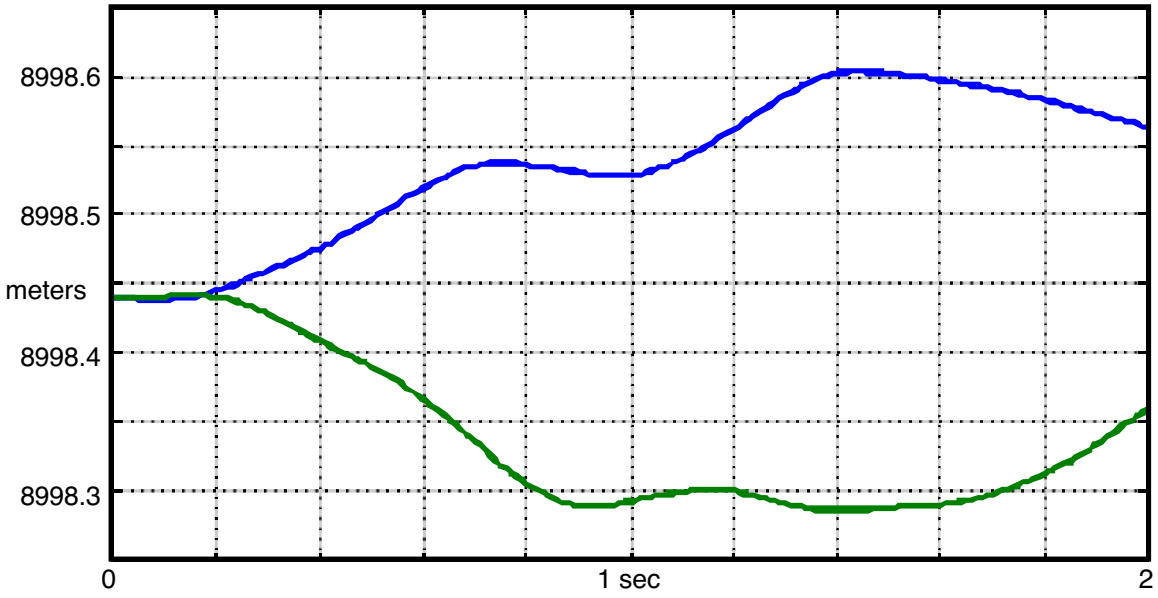

Figure 2-5. Platform Altitude Tracks in Turbulence (0.1 g rms per axis).

In Figure 2-6 we plot the relative path phase deviations from linear phase (i.e. constant Doppler shift), in units of cycles at 300 MHz (UHF), for each platform and for the differential path phase (FDOA phase error), for the scenario geometry shown in Figure 2-2. The differential phase deviation is less than about 15 degrees RMS, which results in a correlation decoherence loss of about 0.6 dB in this case.

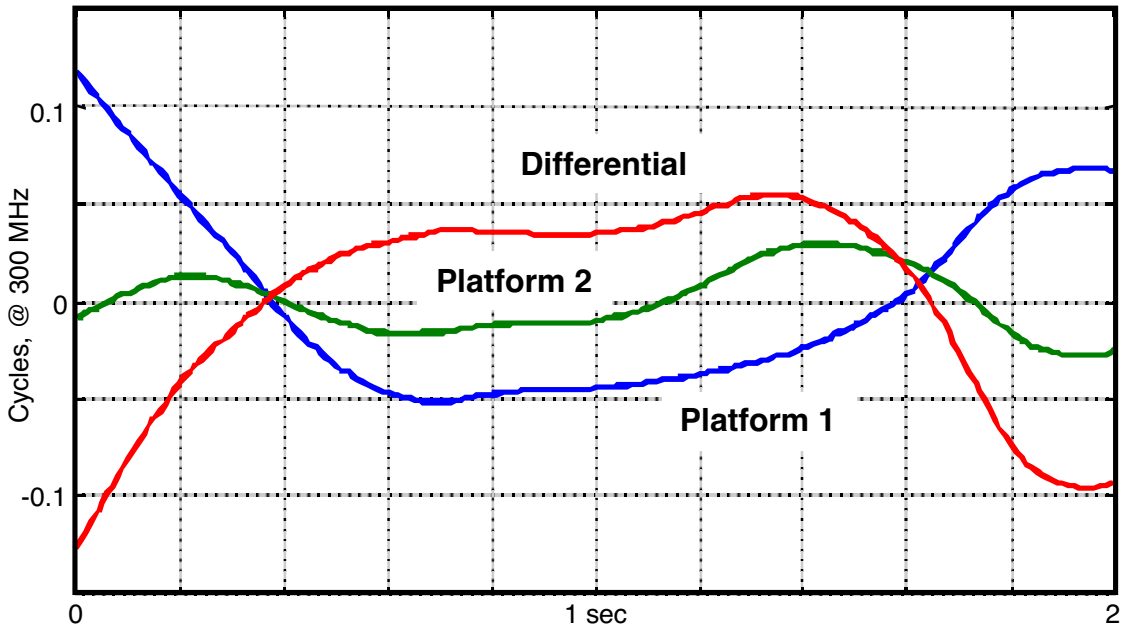

Figure 2-6. Platform Path Phases, Straight Flight in Turbulence (300 MHz).

Motion compensation will both reduce that loss and, more importantly, remove the FDOA measurement biases that arise from the linear phase ramp component, and/or from signal power variations over the nominally two-second collect.

2.3 LPI Fine-Geolocation with Motion Compensation.

The LPI fine-CAF precision geolocation algorithm developed during Phase 0 was updated to incorporate motion compensation and tested via functional simulation of the beamformer short-term CAF peak delay, doppler locations and complex magnitudes.

The fine-CAF performance was evaluated for full-band VHF and UHF LPI signals as observed through a fixed-tuned receiver with only partial band coverage, in order to verify the ambiguity resolution capability of the approach with partial-band intercepts in strongly platform-dynamic environments. The uncompensated and motion-compensated results are compared to demonstrate the effects of platform motion and motion compensation on the LPI geolocation algorithm.

2.3.1 VHF Full-Band LPI Processing with Partial-Band Stare

The LPI algorithm was tested for a two-second collect at a center frequency of 60 MHz and channel bandwidth of 10 MHz, and assuming a 10% intercept duty factor for a wideband VHF LPI signal. The intercept beamformed SINR was assumed to be respectively 6 dB and 9 dB at the two platforms. The target and initial platform geometry is the same as that shown in the coarse-geo illustration of Figure 2-2. One platform is turning at 3 deg/sec in mild turbulence (0.05 g rms per axis), and the other is flying straight in moderate turbulence (0.1 g rms per axis).

The doppler phase deviations from linear (constant frequency shift) are shown in Figure 2-7 for each platform and their differential (FDOA motion phase error). The dominant decohering effect

is the doppler chirp due to the constant-turn-rate acceleration of Platform 1. The differential path phase decoherence amounts to about 0.1 cycles rms at the 60 MHz channel center (doppler reference frequency), for a coherence loss of about 4 dB.

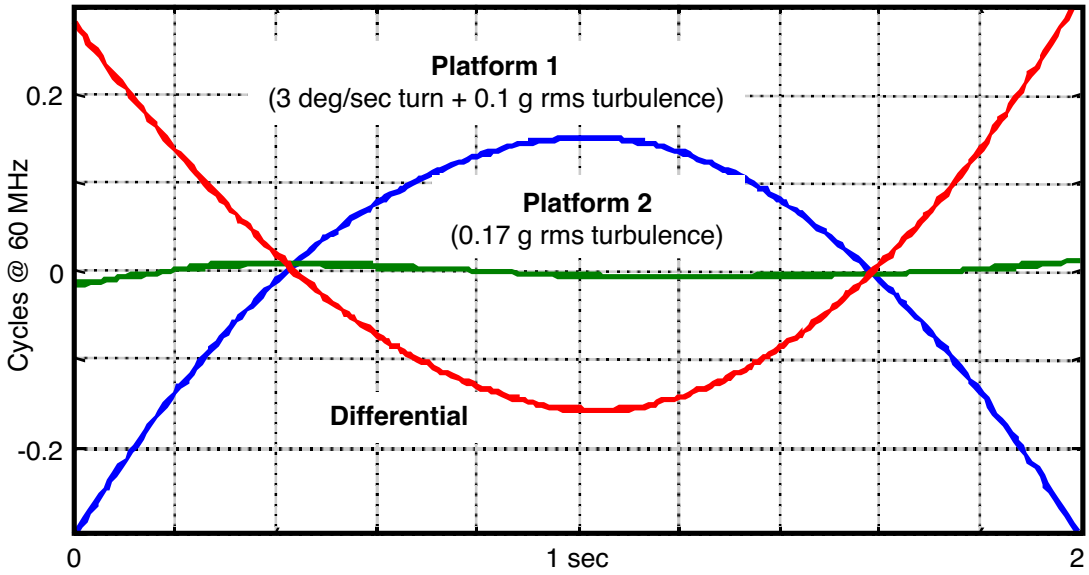

Figure 2-7. Platform Path Phases at 60 MHz.

The long-term, wideband coherent CAF surface without motion compensation is shown in Figure 2-8, with an "X" overlaid at the detected CAF peak and an "O" at the delay and doppler corresponding to the true target location. The CAF delay and doppler search area is defined by the coarse (short-term CAF) delay and doppler measurements and a multiple of their measured standard errors (set to 5x, for this test).

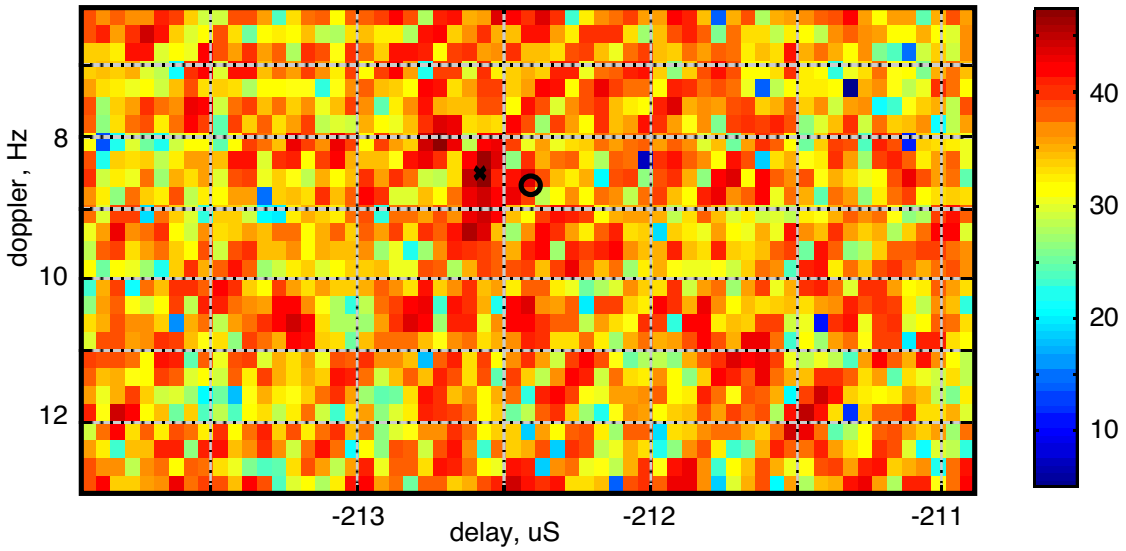

Figure 2-8. Uncompensated CAF Surface, Unnormalized (VHF, 60 MHz).

The bias error in the measured peak location is due at least in part to the irregular power distribution of the inband component of the signal, coupled with the platform motion. The

ambiguous peak amplitude differential is also rather low due to the low duty factor of the signal intercept (low processed bandwidth to signal bandwidth ratio).

The same CAF surface is presented again in Figure 2-9, represented as the (inverse, in dB, of the) normalized mean-square error (NMSE) residual relative to a perfectly correlated CAF. The peak NMSE value of –2 dB corresponds to the coherence loss of 4 dB predicted by the path phase variations.

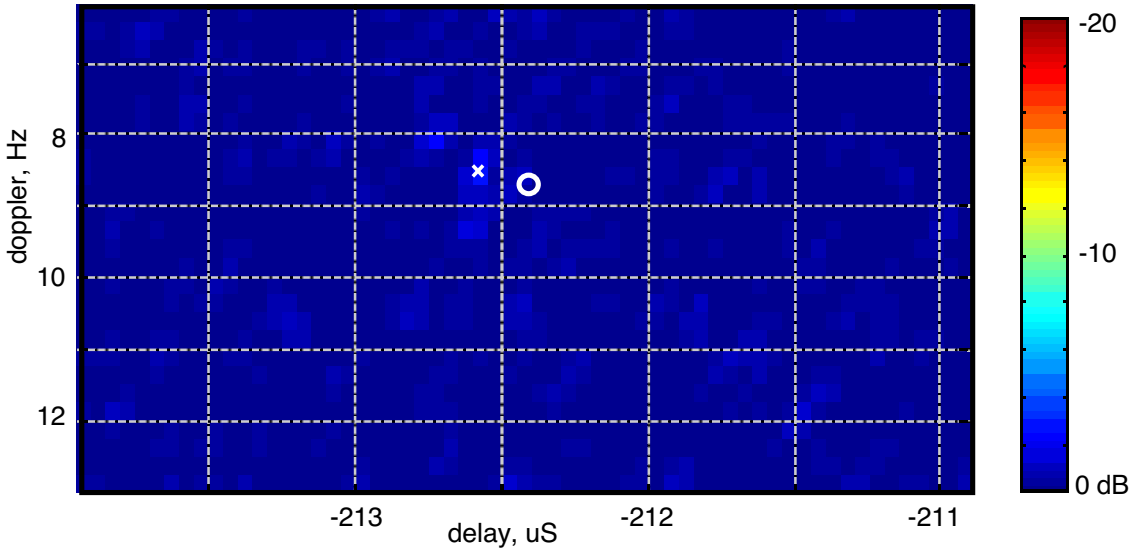

Figure 2-9. Uncompensated CAF Surface, Normalized Correlation Error (VHF, 60 MHz)

The normalized (NMSE) surface for the motion-compensated CAF is shown in Figure 2-10. The coarse delay and doppler obtained from the average short-term CAF data, which was used to determine the delay-doppler spread for the uncompensated CAF above, was converted to target location to define the motion-compensation cue point. The CAF peak is much narrower and the NMSE is down to –8 dB, due to the improved signal coherence after motion compensation.

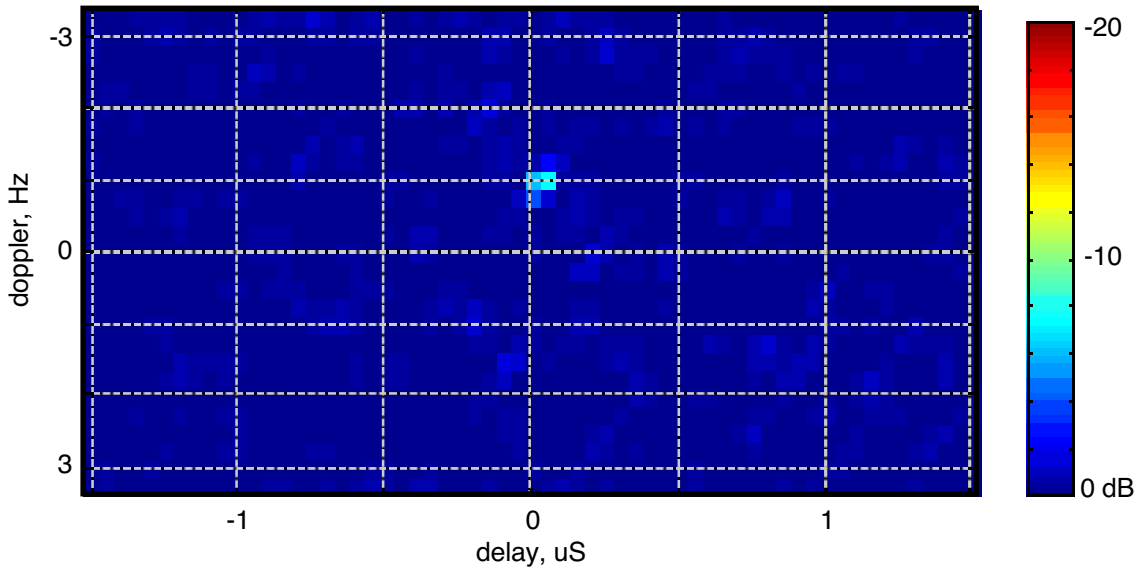

Figure 2-10. Motion-Compensated CAF Surface, Normalized, Iteration 1 (VHF)

The compensated CAF peak location yields the delay and doppler offset between the cue point and the signal data. This offset is converted to location offset via the delay and doppler gradient functions at the cue point to compute a new cue point, at which the motion compensation process is iterated in the CAF NMSE surface of Figure 2-11. This surface shows a peak delay doppler offset of zero, and a CAF NMSE of –10 dB. This process can be iterated as many times as required, and two such iterations have been found to be adequate in all cases studied thus far.

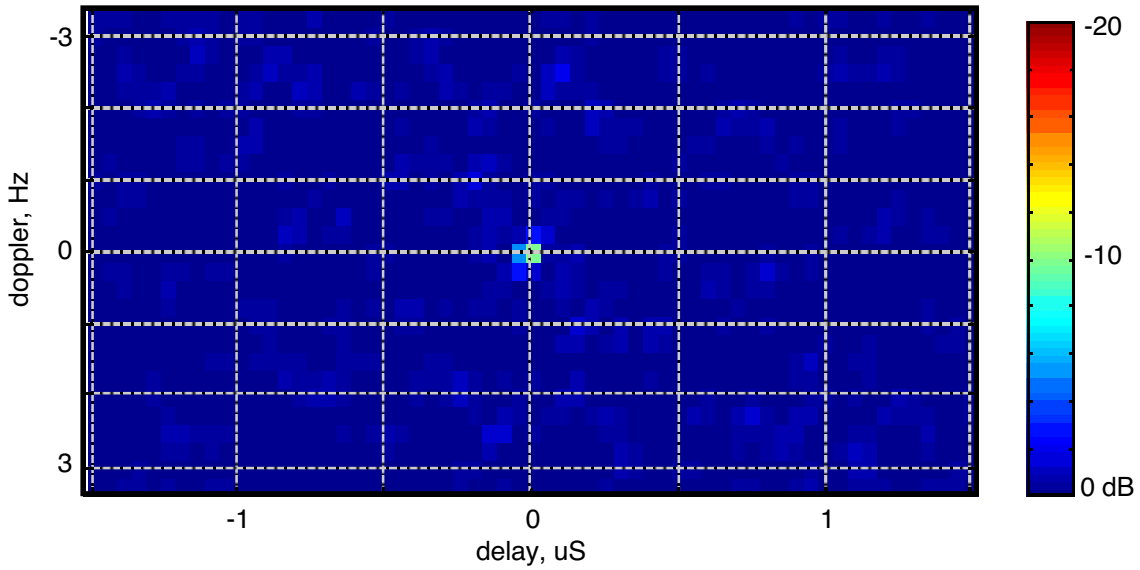

Figure 2-11. Motion-Compensated CAF Surface, Normalized, Iteration 2 (VHF)

It was also found that the conversion from delay-doppler offset to location offset can be markedly improved by iterating on the computation of delay-doppler gradients. These iterations are equivalent to adding the delay doppler offsets to the average delay-doppler values implied by the cue point and average navigation data (platform positions and velocities) and converting to

target position via the same modified Gauss-Newton approach as used for coarse TDOA-FDOA geolocation. This method appears to converge with a single motion-compensation iteration in cases studied thus far, but for the near term Phase 2 implementation we will probably implement both methods for purposes of further comparison and evaluation.

The results of this platform motion and motion compensation analysis for the VHF case are shown in Table 2-2. The miss distances are given for the coarse geolocation cue-point and fine CAF, without motion compensation and for two motion compensation iterations.

Table 2-2. Full-Band VHF-LPI, Partial-Band Intercept Location Results

Location Algorithm	Miss Distance
coarse cue (short-term-CAF averages)	30 km
fine-CAF, uncompensated	2.6 km
fine-CAF, motion-compensated, iteration 1	22 m
fine-CAF, motion-compensated, iteration 2	20 m

The initial location cue is fairly accurate in delay but very coarse in doppler due to the short coherent integration time used for the short-term CAF, which accounts for the large initial miss distance. Even with this large of an initial cue-point offset error, the motion compensation algorithm converges in one iteration.

The miss distances calculated here represent only the errors due to receiver noise and platform motion effects. Additional errors should be expected due to navigation (position, velocity) offsets, reference timing and oscillator phase noise and other effects, which had already been quantified for the LPI geolocation algorithm under the Phase 0 Study.

2.3.2 UHF Full-Band LPI Processing with Partial-Band Stare

The same scenario was used to simulate the LPI processing at UHF, with a channel center frequency of 300 MHz and bandwidth of 20 MHz, and again assuming 6 dB and 9 dB beamformed SINR at each platform and a 10% intercept duty factor for the wideband UHF LPI. The path phase decoherence is therefore increased by a factor of five from the VHF case, to about 0.5 cycles RMS. The uncompensated data is essentially noncoherent, and the fine-CAF surface, shown in Figure 2-12, is noiselike with no dominant peak.

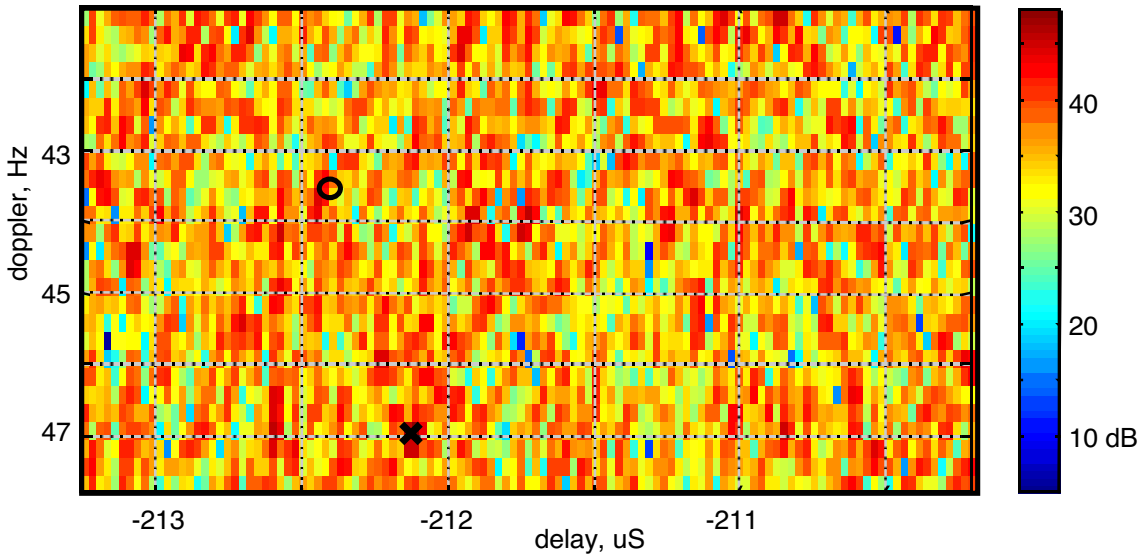

Figure 2-12. Uncompensated CAF Surface, Unnormalized (UHF, 300 MHz).

The uncompensated CAF NMSE surface is shown in Figure 2-13, and confirms the complete lack of discernable signal coherence across the data collect.

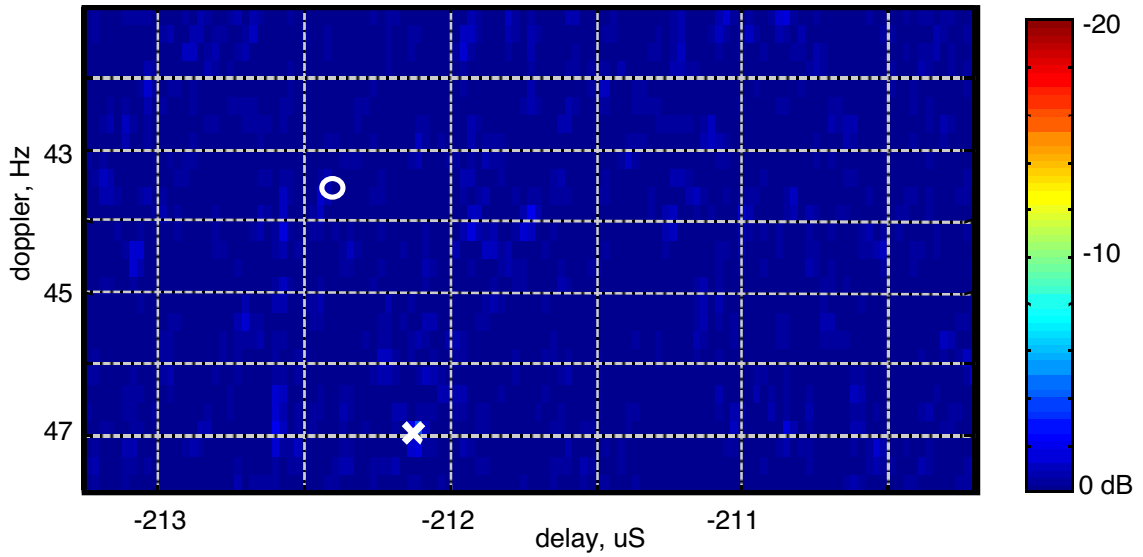

Figure 2-13. Uncompensated CAF Surface, Normalized Error (UHF, 300 MHz)

In contrast, the motion-compensated CAF surface shown in Figure 2-14 has a strong correlation peak with a correlation NMSE of –8 dB, starting from the coarse geolocation cue point obtained by averaging the short-term CAF delay-doppler measurements and platform navigation data.

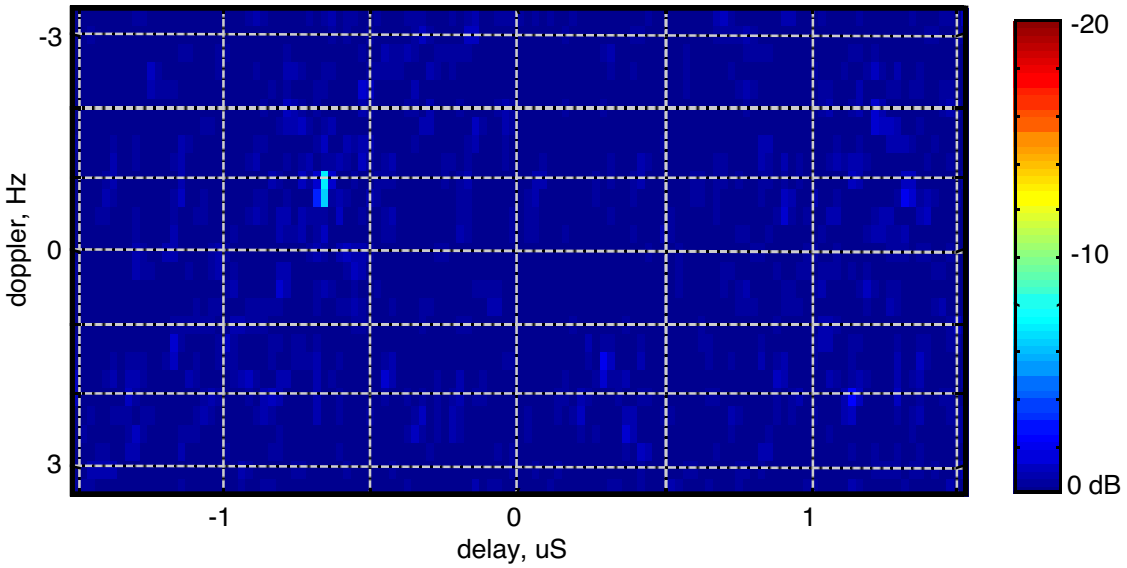

Figure 2-14. Motion-Compensated CAF Surface, Normalized, Iteration 1 (UHF)

After measuring the delay-doppler offset and converting to cue-point location offset and iterating the motion compensation at the updated cue-point, the CAF peak sharpens significantly as seen in Figure 2-15, and yields a correlation NMSE of better than –20 dB.

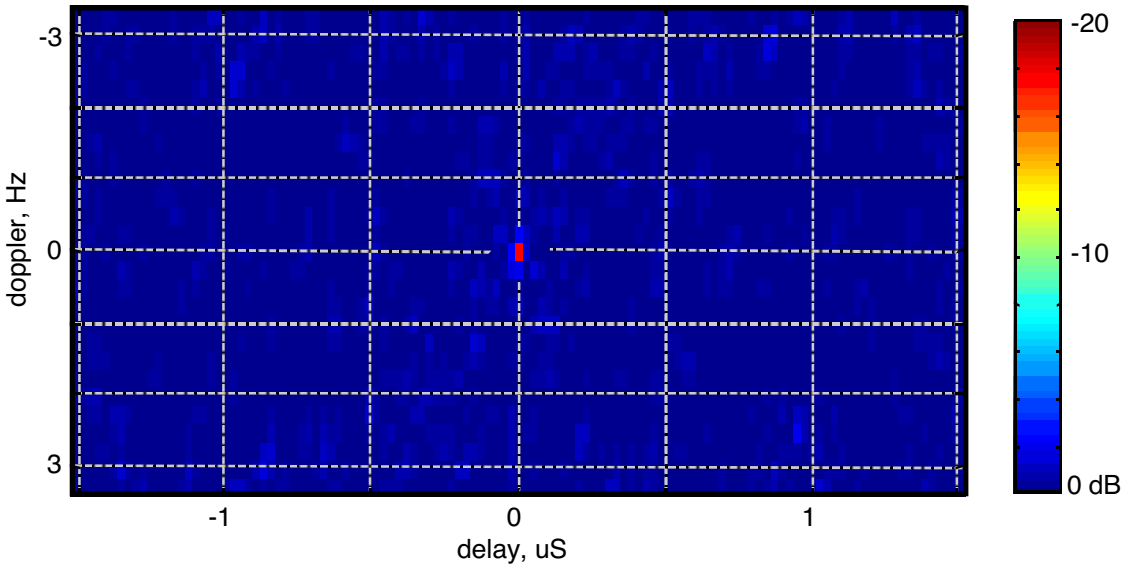

Figure 2-15. Motion-Compensated CAF Surface, Normalized, Iteration 2 (UHF)

The results of this platform motion and motion compensation analysis for the UHF case are shown in Table 2-3. The miss distances are given for the coarse geolocation cue-point and fine CAF, without motion compensation and for two motion compensation iterations.

Table 2-3. Full-Band VHF-LPI, Partial-Band Intercept Location Results

Location Algorithm	Miss Distance
coarse cue (short-term-CAF averages)	5 km
fine-CAF, uncompensated	–
fine-CAF, motion-compensated, iteration 1	9 m
fine-CAF, motion-compensated, iteration 2	14 m

The initial location cue is fairly accurate in delay but coarse in doppler due to the short coherent integration time used for the short-term CAF, although more accurate than in the VHF case by a factor of about 5 as expected due to frequency scaling. Again, the motion compensation algorithm converges in one iteration. The larger miss distance of the second iteration is just an artifact; the x-y errors are actually a closer fit to the theoretical geolocation error ellipse.

3. PinPoint Phase 1, 2 Demonstration Algorithms

The PinPoint Phase 1 and Phase 2 demonstrations have been rescoped to provide beamforming and precision geolocation for conventional signals only, in the interest of accelerating the initial flight tests. LPI beamforming and precision geolocation will be flight-tested during Phase 3. The primary reason for this deferral is that LPI processing requires a much more comprehensive and software-intensive detection and beamforming front-end than is required for preliminary testing of the geolocation algorithms for conventional signals, and it has become incumbent upon the PinPoint program to develop its own detect/beamform front-end capability for purposes of flight testing.

The Phase 2 flight tests are scoped to fully support testing of the geolocation algorithms for conventional signals while minimizing the requirement for additional front-end software. A high-level functional block diagram of the Phase 2 demonstration system is shown in Figure 3-1.

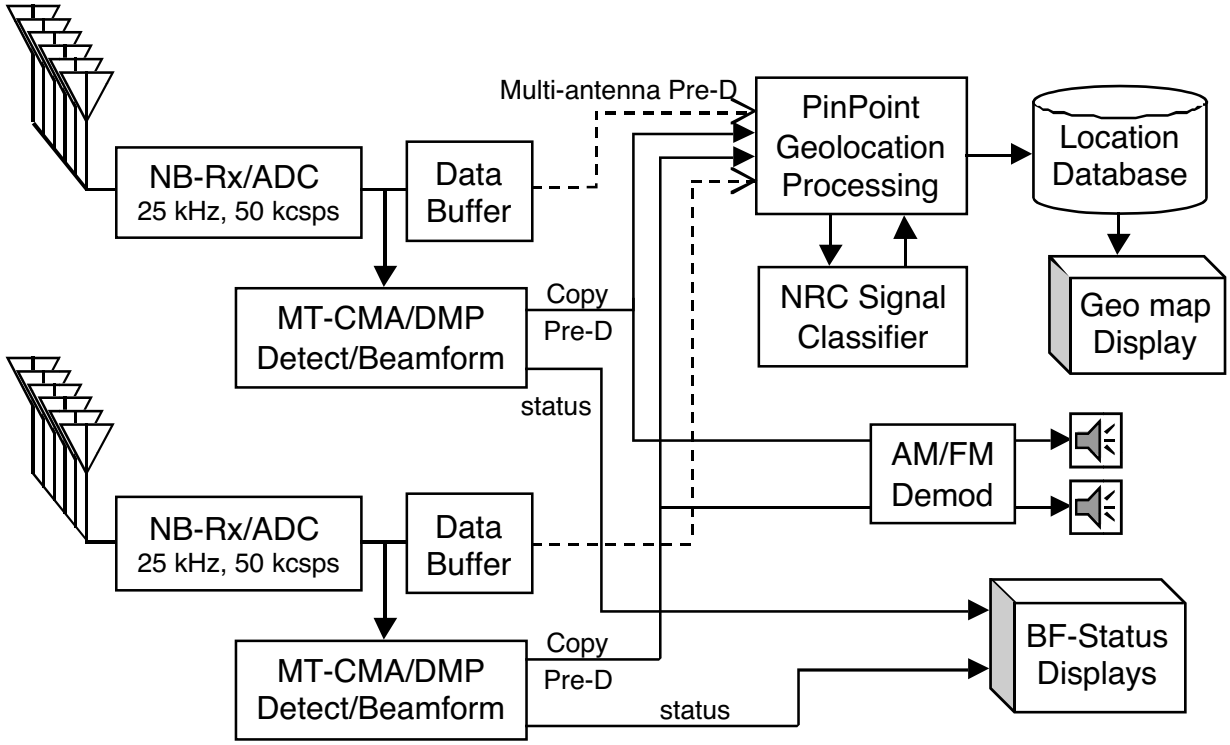

Figure 3-1. PinPoint Phase 2 Demonstration System Functional Diagram.

The receiver front-end in each platform is narrowband and fixed-tuned to the a-priori known frequency channel of a conventional signal net, through the use of digital tune-filter-decimate downconverters. The net is copied beneath co-channel interference through beamforming at both platforms. The beamformer is augmented with edge detection for rapid initialization upon signal-ups, and subsequent cueing of collects for geolocation processing. A deep memory buffer of the multi-antenna narrowband data is retained to allow look-back snapshot acquisition and archival

for offline geolocation processing in cases where one platform detects and beamforms a signal, but the other platform does not.

Snapshots are collected and sent to the PinPoint processor for automatic geolocation of each signal-up detection. The nominal (and minimum-allowed) snapshot collect duration is under operator control. Additionally, the operator can monitor the beamformers and may manually cue snapshot collects for geolocation of active ports (beamformer ports that are locked onto a constant-modulus signal).

The snapshots are received by the PinPoint processor and correlated for uncompensated geolocation (as well as verification that the same signal is being received by both platforms) and then iterated for motion-compensated geolocation. Geolocation results are then forwarded to the Geolocation Display processor for incorporation into the location database and display as an overlay on the PinPoint display maps.

We envision integrating the Nonlinear Resonance Classifier (NRC) with PinPoint for the Phase 2 flight tests. This integration should be straight-forward since both processes require similar-duration snapshots. In this event, the NRC results will be incorporated into the geolocation records in the location database.

It is also highly desirable to also have at least a rudimentary demodulation capability to provide audio for emitter identification and verification purposes. This capability is currently envisioned to support only analog FM and AM, but could be extended if necessary to include unencrypted digital modulations such as FSK. The intent is to provide demodulators for the radios used as test emitters in the Phase 2 flight test, in order to positively associate detections with particular test radios through manual voice recognition.

An important simplifying feature of the Phase 2 demonstration concept is the elimination of DF, and with it, the requirement of DF array calibration flights and cal-verify software. Without DF, however, we have to either simulate DF cues using a-priori locations and a tightly scripted test, or employ coarse area-of-interest cuing only and deal with the potential for TDOA-FDOA ambiguities by controlling the scenario geometry.

3.1 MT-CMA / DMP Detect and Copy Beamformer

The PinPoint beamformer algorithm is shown in the block diagram of Figure 5-4. This algorithm is a reduced-complexity version of the Radix-Proprietary GBC algorithm. The weights adaptation is based on the Constant Modulus Array algorithm, and is augmented with signal-up and signal-down edge detection based on the Dominant-Mode Prediction algorithm. The up-edge detector is used to initialize the beamformer weights and cue a copy collect for geolocation. The down-edge detector is used to terminate the collection in cases where the signal duration is shorter than the desired collect interval.

The beamformer is phase-stabilized with a proprietary, IRAD-developed algorithm in order to preserve phase coherence for fine doppler measurements over a collect duration that spans multiple beamformer weights update intervals.

The beamformer lock statistics are passed out for beamformer status monitoring. An operator might task geolocations of ports that are seen to be locked via this statistic, either to verify the continuation of a previously detected transmission or to geolocate a signal that eluded the signal-up detector by slowly fading in. See Figure 4-9 for an example of the behavior of the beamformer up/down detection and lock statistics over the span several signal emissions.

3.2 TDOA Compensation.

The extent of TDOA compensation needed for PinPoint is dependent on the receivers used and the accuracies required. Typical receivers employ SAW filters to shape the IF passband. These filters have a bulk group delay of roughly 1.5 microseconds that dominates the group delay of the receiver and can vary from device to device and with changes in temperature. SAW filters also exhibit ripples in the passband response that yield a frequency-dependent group delay over narrow bandwidths that can vary over frequency and across receivers by roughly ±30 nsec or more, depending on the device type.

In many cases, the group delay variation across receivers that have been warmed up to a stable operating temperature can be as little as 100-200 nsec. In a temperature-controlled environment such as a laboratory or even a pressurized, heated cabin in an airplane, the bulk group delay of the receivers may be repeatable enough to provide sufficient timing accuracy for acceptable flight testing without the use of dynamic calibration. A measurement of the overall differential group delay might be made by geolocating an emitter of known location and measuring the differential timing error.

For the highest accuracies, however, as well as robustness of operation in a temperature-varying environment, we require dynamic receiver TDOA compensation. A precisely modulated waveform is injected into the receiver front-ends and the outputs are correlated with the known waveform paradigm. The receiver group-delay measurements are used to select a set of delay-compensating FIR filters, one for each narrowband receiver channel. In Phase 2, this TDOA compensation will be implemented by applying these filters to the narrowband data immediately prior to the signal detection and beamformer processing.

The TDOA compensation waveform is generated by modulating a tone generator at the channel center frequency with a known, pseudorandom BPSK bit sequence that is triggered at a known instant in time, e.g. a GPS 1-second time epoch marker, to which the receiver A/D samples are also synchronized. The known BPSK bit sequence is cross-correlated against the A/D samples to generate the receiver impulse response. Multiple responses can be averaged if desired to reduce noise, or perhaps examined spectrally via FFT across the measurements (slow-time axis) to quantify the channel response stability over time.

3.3 PinPoint Geolocation Processing, Both Platforms Copy

The PinPoint algorithms for post-beamformer geolocation of conventional signals are described in the block diagram of Figure 3-2. At this level of presentation, we assume that beamformed snapshots are acquired from two platforms and are already associated with each other, i.e. both beamformers are copying the same signal. Ordinarily, for detection-driven geolocation, this

assumption is reasonable since the association is made implicitly based on frequency and time-up coincidence. The algorithm can be extended to allow geolocation of coincident beamformed signals by associating pairs based on correlation strength.

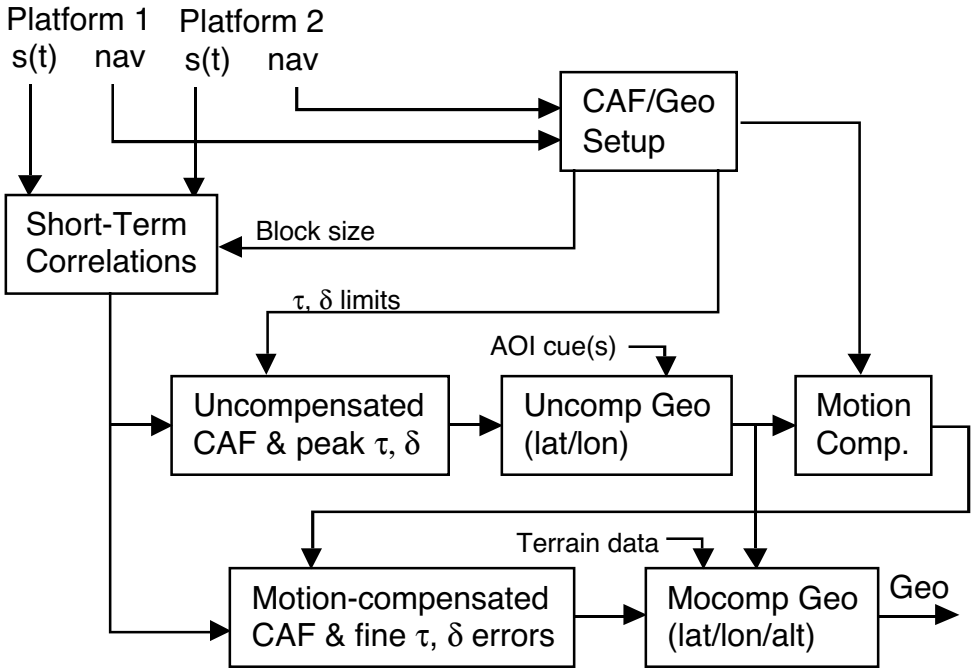

Figure 3-2. PinPoint Geolocation for Conventional Signals, Both Platforms Copy.

The primary inputs required for PinPoint processing include the beamformed copy pre-D collects from each platform, precise collect timing and channel frequency offset, and the navigation data for both platforms over the duration of the snapshot.

If terrain elevation data is available it can be used in the final motion-compensated geolocation calculations, otherwise target latitude and longitude is computed at an operator-provided reference elevation (e.g. the mean terrain height over the area of interest). Finally, since DF is not available for geolocation cuing and ambiguity resolution, an Area of Interst (AOI) cue point must be specified, and the platform geometry should be arranged to provide unambiguous TDOA-FDOA over the AOI.

Other inputs include algorithm-control parameters such as coarse CAF coherent processing block size, delay and doppler resolution and oversampling, initial Area-of-Interest (AOI) cuepoint(s), and occasional snapshots of TDOA compensation data.

A preliminary, uncompensated CAF is computed to unambiguously cover the full range of delays and dopplers possible for a stationary target in the plane best fitting the platform positions and velocities, and with doppler offset and sampling rate sufficient to provide low integration loss across the AOI. The required delay-doppler spread is computed prior to CAF computation from the platform nav data, averaged over the collect. The computed CAF surface is then peak-detected for an uncompensated delay-doppler estimate. This delay-doppler estimate is converted to target position via modified Gauss-Newton (MGN) iterations from a starting point nominally

in the center of the AOI. The resulting coarse geolocation is used with the platform nav data to compute the motion compensation delay and doppler phase corrections for fine geolocation.

Fine geolocation is performed by recomputing the CAF surface with motion compensation to the coarse-geolocation cue point. The data is compensated with the coarse doppler offset corresponding to the cue point, and the short-term correlations are fine-compensated for variation in doppler phase and delay according to the platform flight track variations during the collect as determined from the navigation data. The effect of this motion compensation is to offset the CAF peak to zero delay and doppler for a signal at the cue point, and also to focus the peak to minimize its delay and doppler spread. The measured peak delay and doppler offsets are then converted to x-y offsets in the horizontal plane at the coarse geo point to generate the fine geolocation.

The fine geolocation process can be iterated, using one fine geo as the cue point for the next. In the simulations performed to date we found little actual miss-distance reduction from such iteration, but it is easily implemented with relatively low additional computational complexity, and the iteration results give the engineer a reassurance that convergence has been reached.

3.3.1 CAF/Geo Setup.

The Cross-Ambiguity Function (CAF) surface is derived from a sequence of short-block cross-correlations between the two beamformer snapshots, where each correlation is computed via FFT, conjugate-multiply and inverse-FFT. The purpose of computing this surface is to determine the relative delay and frequency offset (doppler shift) between the two beamformer paradigms. this delay and doppler offset is then converted to lat-long through knowledge of the platform positions and velocities.

3.3.1.1 AOI Cue

The area of interest may be geographically limited, or there may be other a-priori information such as an LOB triangulation that localizes the target and limits the required search area. These geographical limits can be transformed into delay and doppler search ranges over which the CAF surface must be computed. However, a potential target could be submitted for geolocation processing that is not within the defined area of interest, or for which a wild bearing was used for triangulation cuing. We would nominally expect to be able to recognize that event by either finding that the maximum correlation amplitude was on the edge of the computed CAF region, or that the measured CAF peak amplitude was not commensurate with the presumed signal SNR. In those cases we would either reject the geolocation or revert to a full-area CAF.

For demonstration purposes, we will probably want to use full-area CAF most of the time, at least initially. Also, there is some concern that correlations from residual interferors located outside the area of intersest might alias into the CAF, biasing the results. This error is minimized by always performing doppler-unambiguous, full-area CAF processing.

In general, the transformation from target location to differential delay and doppler can be ambiguous; i.e. a given CAF peak location (delay-doppler) can arise from multiple (usually at most two) locations. The conversion from delay-doppler to target position is most easily

accomplished via modified Gauss-Newton (MGN) iterations. Other approaches can be taken that are robust enough to find all ambiguous locations, but they are considerably less convenient to implement. The MGN approach is readily implemented and applies directly to fielded applications where LOB-triangulation is available for initialization. For that reason, our nominal approach for demonstration is to employ MGN from a fixed starting-point, nominally in the center of the area of interest, and to control the platform geometry to yield an unambiguous transformation in the vicinity of the test targets. If necessary, we could expand the approach to repeat the MGN computation from multiple initial points in order to identify ambiguities.

3.3.1.2 Delay, Doppler Limits

Upper bounds on the delay and doppler spread can be easily computed from the platform positions and velocities. The maximum delay spread is twice the platform separation, and the maximum possible doppler velocity spread is twice the sum of the platform velocities:

$$|\tau| \leq \frac{|\mathbf{P}_2 - \mathbf{P}_1|}{c}$$

$$|\delta| \leq \frac{|\mathbf{V}_1| + |\mathbf{V}_2|}{\lambda}$$

The delay limits are sharp in that the limits are achieved, by targets near the horizon aligned with the platform baseline. However, the doppler limits are not sharp, and in most scenarios the actual doppler spread is less by as much as a factor of two or more.

Sharp doppler limits can be readily calculated for a planar geometry, which is a good approximation for the baseline PinPoint applications. It can be shown that the doppler extrema must occur either at the boundaries of the plane punctured at the two platform positions (i.e. on vanishingly small circles about each platform and a circle of unboundedly large radius representing the boundary at infinity) or at the point of intersection of the two lines defined by the platform positions and velocity vectors. Simple formulas are readily generated for the local extrema on each circle and at the single interior point. The global extrema are then obtained as the minimum and maximum of the computed local extrema.

If the CAF is to be restricted by an LOB triangulation cue, we can convert estimates of LOB uncertainty into an error ellipse in Local-ENU x-y, and then (via the Jacobian of the x-y to delay-doppler transformation) into an error ellipse in delay-doppler, from which delay and doppler ranges can be derived.

3.3.2 Short-Term Correlations

The data block size used for computing the CAF surface need not be related in any way to the beamformer update intervals, which in turn need not be the same between platforms. In dynamic environments where one platform or the other is turning or undergoing turbulence, it may be desirable to set the beamformer update intervals independently to maximize performance.

The CAF is computed by generating a sequence of short-block cross-correlations over the required delay spread and then coherently integrating the correlation lags across blocks via FFT

to generate a doppler spectrum at each lag, as illustrated in Figure 3-3. The data blocks are overlapped by an amount at least equal to the delay spread, $2\Delta\tau$, and have a nonoverlapped interval of length $\Delta T \leq 1/\Delta F$, where ΔF is the required unambiguous doppler spread.

For dopplers at the edges of the unambiguous range ($\pm\Delta F/2$) the correlation loss due to doppler frequency mismatch is about 4 dB. For uncued full-area CAF, the block size should be reduced by a factor of two ($\Delta T = 1/2\Delta F$) so that the correlation loss at the doppler edges ($\pm\Delta F/2$) is held to 1 dB.

The block size may also be constrained so that the sum of its duration plus the required delay spread, in data samples, is a power of two (or slightly less, which is equivalent to computing a somewhat wider delay spread than was required).

In order to give an indication of the general scope of the block sizing parameters we expect, the block sizes for a fully unambiguous delay and doppler CAF for typical platform parameters are presented in Table 3-1. The platform velocities are assumed to be 180 kt = 90 m/sec, and the baseline is 180 km for a delay spread of ±0.6 mSec = 1.2 mSec total. The paradigm sample rate is assumed to be 50 kcsps, and the doppler spread crude upper bound given by the sum of the velocity vector norms is used to determine the maximum allowable carrier frequency at each power-of-two block size.

Table 3-1. Carrier Frequency vs Block Size for Unambiguous CAF Doppler

FFT points	ΔT, mS	$\Delta T/(\Delta T+2\Delta\tau)$	max-f_0, MHz
128	1.36	0.53	613
256	3.92	0.77	213
512	9.04	0.88	92
1024	19.28	0.94	43

The blocks are overlapped by $2\Delta\tau$ = 1.2 mS, and the resulting non-overlapped interval ΔT is given. The ratio of nonoverlapped interval to total block size is given as an indication of the numerical efficiency of the block FFT-multiply-FFT correlation processing. Note that the efficiency goes down as the carrier frequency goes up, unless the delay spread can be reduced. One way to improve efficiency at higher frequencies in the uncued case is to compute multiple CAFs over short nonoverlapping ranges of delays, and concatenate the results across delay. For the purposes of Phase 2 experiments, we can forego such complications simply by limiting our tests to the VHF and UHF tactical bands (below 400 MHz).

3.3.3 Uncompensated CAF.

The Cross Ambiguity Function (CAF) of the beamformed data is computed efficiently in the frequency domain using FFT-based correlation processing. In summary, short-block cross-correlations are performed by FFT, conjugate-multiply and inverse-FFT to generate a time series of correlation lag coefficients spanning the range of unknown differential delay (TDOA). The time series for each lag is then analyzed by FFT to break it into differential-doppler (FDOA)

components. The resulting TDOA-FDOA surface is then peak-detected to determine the signal differential delay and doppler components, and optionally displayed as an engineering display.

The CAF computation algorithm is shown in Figure 3-3, and is described as follows:

- Apply the coarse doppler compensation to one paradigm. The doppler compensation frequency is ordinarily set to the center of the initial location cue or area of interest, to maximize processing gain in the a-priori vicinity of the SOI.
- Time-align the other paradigm to remove any average delay offset between them.
- Segment the paradigms into time-aligned blocks, with overlap at least equal to the required CAF delay spread ($2\Delta\tau$), and non-overlapped interval (ΔT) no greater than the inverse of the full-horizon-area doppler spread (for unambiguous doppler) and half the inverse of the area-of-interest doppler spread (for low processing loss over the AOI). The total block length should be a power of two samples long. One of the paradigms is zeroed out over the block overlap region, so that in fact its data is not overlapped but instead has leading and trailing zeros.
- FFT the data blocks, both paradigms. Conjugate one of them, multiply them, and FFT the result, to get the short-term cross-correlation function as follows:

$$C_{xy}(\tau) = \frac{1}{T}\int_0^T x(t-\tau)\, y^H(t)\, dt = \frac{1}{F}\int_{-F/2}^{F/2} X(f)\, Y^H(f)\, e^{-i2\pi f\tau}\, df$$

$$\text{where} \quad X(f) = \frac{1}{T}\int_0^T x(t)\, e^{-i2\pi ft}\, dt$$

  Optionally, we can zero-fill and inverse-FFT with twice the FFT size to oversample the delay correlations, for a smoother CAF surface.

- Extract the short-block correlations across the required delay range (symmetric about zero).
- FFT across blocks at each delay. Zero-pad to at least the next higher power of two, to achieve an oversampling of roughly 2x in doppler (e.g. between 1.5x and 3x). Optionally, the samples are weighted prior to zero-fill-FFT with a Hanning or Blackman window to reduce doppler sidelobes.
- Extract the doppler filters closest to band-center, covering the desired doppler display range for the CAF display. The doppler compensation offset may be incorporated into the CAF doppler axis definition if desired.

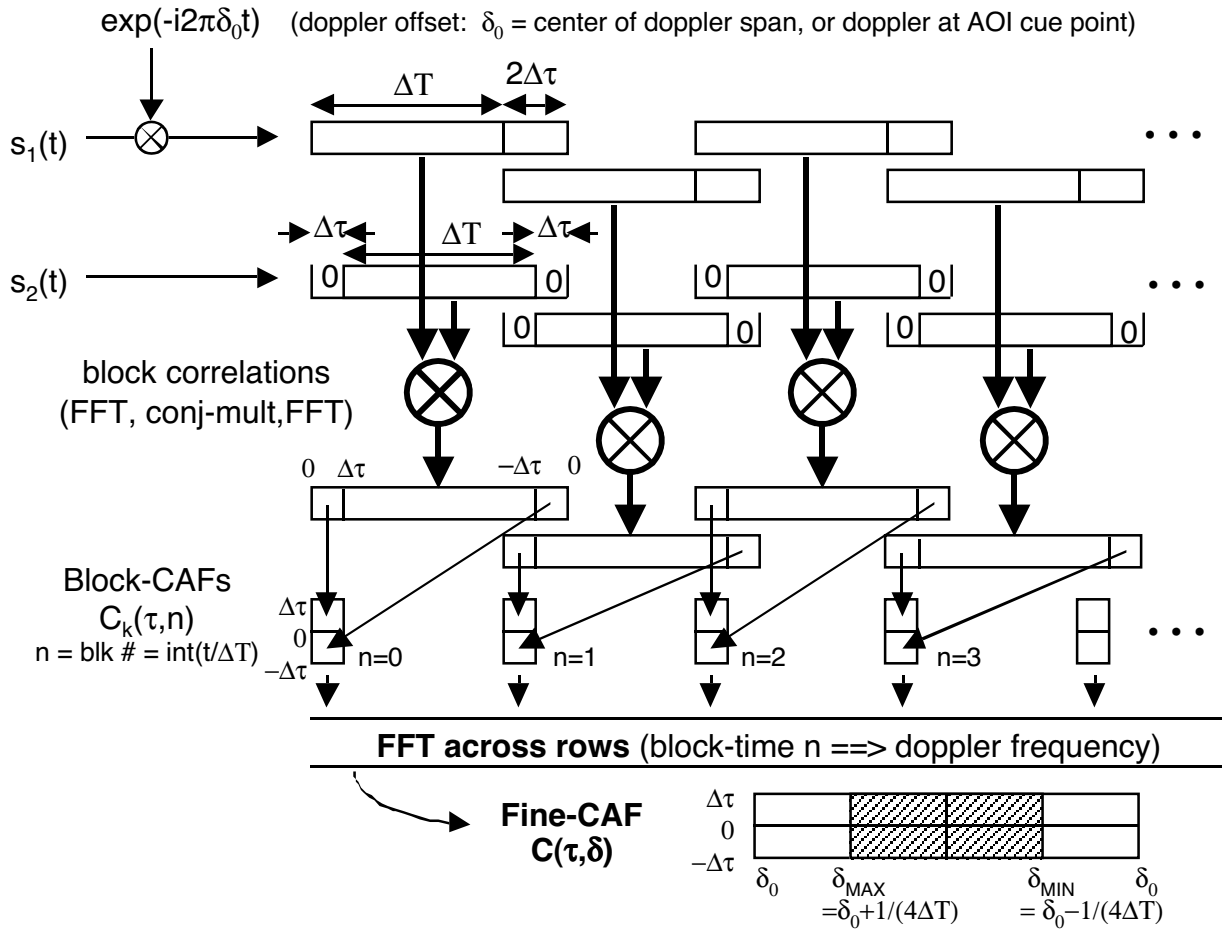

Figure 3-3. Cross-Ambiguity Function (CAF) Computation.

The resulting CAF surface is then magnitude-squared and peak-detected. The peak position is estimated with quadratic interpolation in delay and doppler to get the coarse delay-doppler measurements for coarse geolocation.

3.3.4 Uncompensated Geolocation.

Geolocation is performed by inverting the transformation from x-y in the plane tangent to the earth at some nominal point as defined by the "Local East-North-Up" coordinate system (Local-ENU) to differential delay-doppler, at the delay-doppler measured at the peak of the CAF surface. The forward transformation, from x-y to delay-doppler, is easily defined in terms of the platform positions and velocities (averaged over the duration of the collect) relative to that x-y plane. The transformation is inverted via a modified Gauss-Newton approach using the transformation gradients and starting from a convenient x-y point, e.g. the center of the area of interest. This cue point is used to define the Local-ENU coordinate x-y plane for the first iteration. At each iteration, an x-y correction to the cue point is computed and the z-component is corrected for the nominal curvature of the earth (spherical assumption) to define a new cue point for the next iteration.

At the end of the iterations, the cue point location is converted into latitude and longitude, using the standard oblate-spheroid earth model used for map lat-long definition, and fixed to the surface of the earth at that coordinate according to either digital terrain data for the region or an engineering input representing the average terrain height.

3.3.5 Platform Motion Compensation.

Motion compensation is performed by computing the instantaneous differential delays and doppler phases from the coarse geolocation point to the platform positions at the times corresponding to the short-block CAF cross-correlations of the master paradigm. This computation is conveniently carried out by computing the exact distances between the target cue point $\mathbf{P}_T$ and platform interpolated positions $\mathbf{P}_1(n)$, $\mathbf{P}_2(n)$ at the required time instants, in double precision, and converting into delays and wave-numbers at the channel center frequency f_0:

$$\tau(n) = \frac{\left|\mathbf{P}_T - \mathbf{P}_2(n)\right| - \left|\mathbf{P}_T - \mathbf{P}_1(n)\right|}{c}$$

$$\phi(n) = 2\pi\,\tau(n)\,f_0(n)$$

The delay compensations $\tau(n)$ at each block are implemented as phase ramps across the frequency-domain short-term correlations, with phase offsets across the frequency bin corresponding to f_0 for true fine time-delay motion compensation.

3.3.6 Motion-Compensated CAF/Geolocation.

The CAF is compensated in the frequency domain via applying the conjugate phase ramp corresponding to the compensation time delay at each CAF block, just prior to the final FFT that generates the block cross-correlation functions $C(\tau,n)$ in Figure 3-3. The phase ramp is also phase-scaled to have the compensation doppler phase $\phi(n)$ at the frequency bin corresponding to f_0 for that block. The compensation doppler phase is adjusted to account for the coarse doppler compensation offset already incorporated into the CAF paradigms.

The compensated CAF is very tightly cued by the coarse geolocation arising from the uncompensated CAF. The actual size of the computed CAF surface can be quite limited, perhaps being computed at only a few delays and dopplers. On the other hand, it may be convenient and in fact desirable for display purposes, to recompute the entire CAF or at least a large portion thereof, to show graphically the effect of motion compensation as a dramatic sharpening of the correlation peak in doppler, particularly during platform turns and/or turbulence. Also, other useful information might be derived from the compensated CAF peak width in doppler, e.g. decoherence effects due to target motion.

3.3.6.1 Fine TDOA, FDOA Errors.

The result of the motion compensations is to shift the CAF surface so that the peak lies at zero differential delay and doppler, and to cohere the data through platform flight path variations, when the target is actually located at the motion-compensation cue point (zero coarse geo error). The dependence of the motion compensation phase variation profiles due to flight path

deviations from ideal position-velocity are slowly varying functions of target position. The dominant effect of a target offset from the cue point (nonzero coarse geolocation error) is a coherent delay and doppler offset of the compensated CAF peak. These offsets are most readily and accurately measured by interpolating the compensated CAF peak position and recomputing the CAF on a sequence of successively finer delay-doppler grids. These fine-search grids can be as small as 5x5 or even 3x3, and are computed directly via DFT rather than oversampled FFT.

3.3.6.2 Motion-Compensated Geolocation.

The delay and doppler errors measured from the Compensated CAF are transformed back into x-y errors at the coarse-geo cue point, in its Local-ENU coordinate system x-y plane, through inversion of the x-y to delay-doppler transformation at the cue point and the nav data (position, velocity) averaged over the collect. The inversion is nominally performed via modified Gauss-Newton iterations using the averaged nav data and adding the fine TDOA-FDOA errors to the computed TDOA-FDOA values at the cue point. The motion compensation process can be iterated if desired, to demonstrate convergence.

4. Phase 1 Demonstration System Development

A high level block diagram for the Phase 1 demonstration system is shown in Figure 4-1. The data simulator, implemented in MatLab, is used to generate test data files. These files are uploaded to the Quad-G4 DSP card and stored in local memory. The DSP card is partitioned into two symmetrical halves, each of which implements the beamforming function for one of the two platforms. The signal detections and beamformed copy data are routed through the Ethernet interface to the Ground Element (the same Sun workstation that will be used in Phase 2 flight testing) for inter-platform data (report) association, geolocation processing and real-time display.

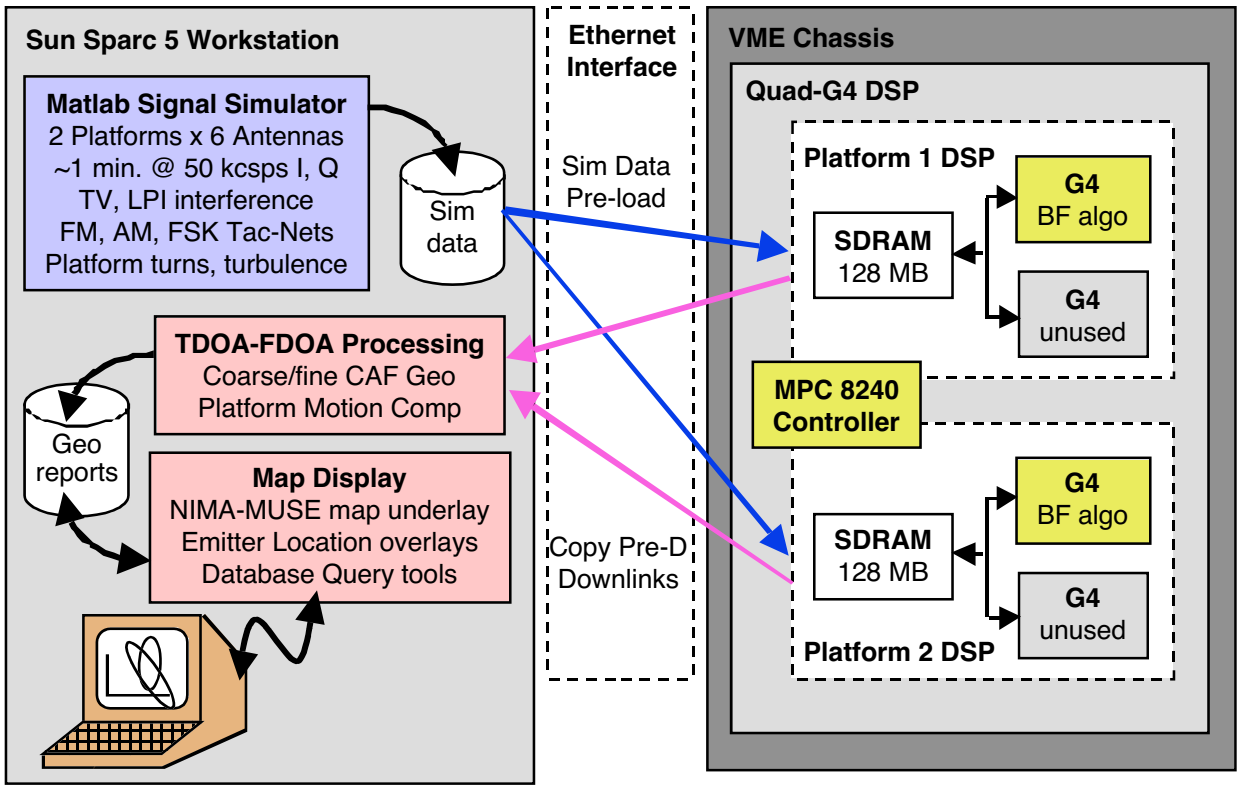

Figure 4-1. PinPoint Phase 1 Demonstration System Block Diagram

In support of the Phase 1 DSP implementation effort, mirror code has been implemented in MatLab in order to provide early performance quantifications, as well as a prototype for both precisely handing off the algorithm details and providing a reference implementation for comparison testing with DSP code.

In addition, a multi-channel, multi-platform data simulation capability was developed that generates up to several minutes of narrowband data and associated navigation data for use in testing and demonstrating the Phase 1 Development system. Various interference sources are simulated, including gaussian noise, broadcast TV, and LPI emitters. Target signal waveforms are generated to simulate temporally overlapping traffic from multiple tactical single-channel conventional nets employing AM, FM Voice or FSK Data modulations. The voice modulations incorporate actual recorded voice cuts in order to accurately represent the syllabic structure of

(English and Spanish language) voice. Dynamic platform motion effects including turbulence, platform turns and roll rates are modeled with high fidelity for the multi-antenna arrays. Similar models are implemented for the individual emitters and can be invoked to model moving-target decoherence effects.

4.1 GeoDisplay HMI and Map Display Software

The purpose of the GeoDisplay HMI software is to provide a means to display and analyze geo-locations produced by the PinPoint demo system. It maintains a file of geo-location reports, plots locations and their associated error ellipses on a map, and provides tools for analysis of the reports. Figure 4-2 shows a functional diagram of the software.

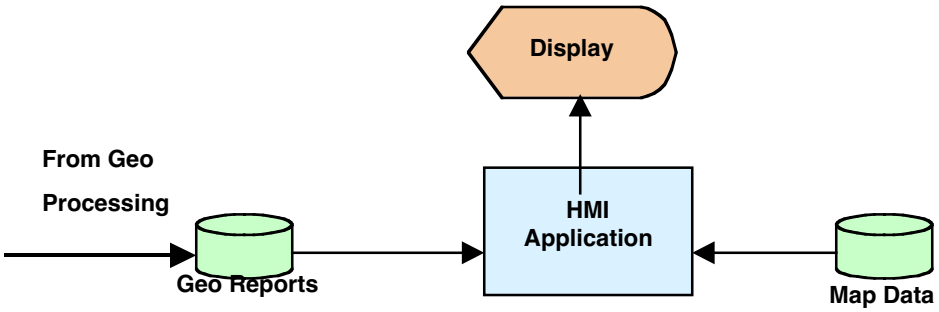

Figure 4-2. HMI Software

The software capabilities and general usage information are given in the following sections.

4.1.1 Map Plotting

The map background is produced by plotting raster maps derived from NIMA (National Imagery and Mapping Agency) map products. Vector overlays of certain map features may be added, also derived from NIMA map products. A preparation step is required to turn the map products into files useable by the PinPoint software. This step is done once for an area of interest, with the NIMAMUSE software, available from NIMA's web site. NIMAMUSE is used to select areas and features from the original CDROM or files containing the map products. The output in the case of raster maps is a NIMAMUSE image file, and is a vector file in the case of vector maps.

NIMA map products for the area around Fort Hood were available as samples over the web, so that area was chosen for a demo scenario. Products downloaded and used included CADRG (Compressed ARC Digitized Raster Graphics) maps in three different scales: Operational Navigation Charts (ONC, 1:1,000,000), Joint Operations Graphics-Air (JOG-A, 1:250,000), and Topographic Line Maps (TLM, 1:50,000), vector maps in two different scales: Vector Map Level 1 and Level 2, and Level 1 and 2 Digital Terrain Elevation Data (DTED). A raster file of imagery in the Controlled Image Base (CIB) format could also have been used as a map background, but data for the Fort Hood area was not available as a sample download.

4.1.2 Program Start-Up

The PinPoint HMI application, called ***geodisplay***, is shown in Figure 4-3. After starting the application, choose Open Map from the File menu. To open the Fort Hood map, choose FortHood.txt. This file contains a list of map files for the Fort Hood area and their relationship (zoom level). The initial map to be displayed is an ONC map which has a scrollable extent of a few hundred kilometers. For a standalone demonstration of GeoDisplay only, choose Open Geo File from the File menu. Select a file containing geo-location reports and the reports will be listed in the text window, and the error ellipses will be plotted on the map.

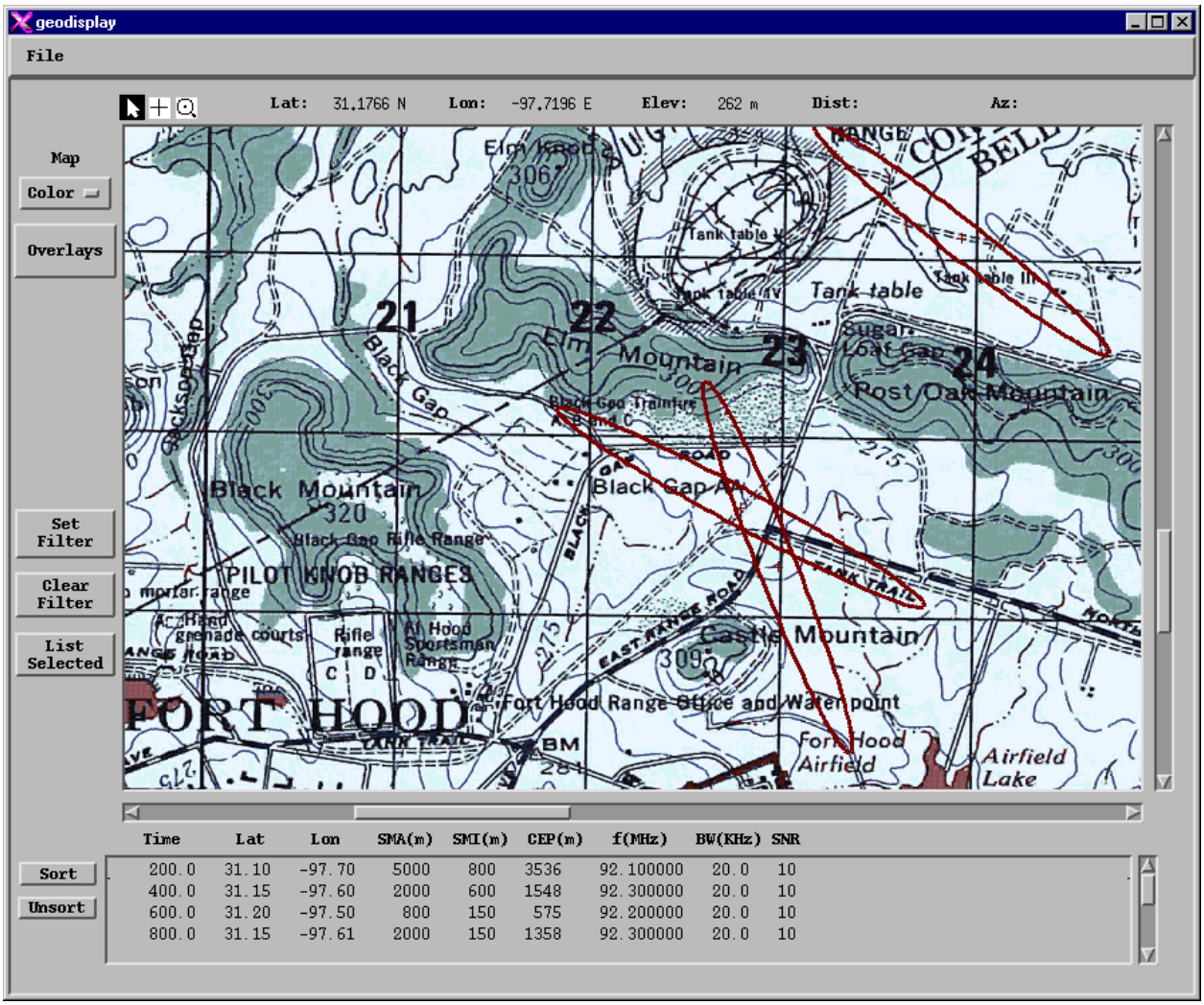

Figure 4-3. "GeoDisplay" Application Interface

4.1.3 Map Readouts and Tools

The readout panel above the map contains a continuous cursor readout of latitude, longitude, and (if available from at DTED file) elevation above sea level. Also on the panel are three tools, Selection, Measurement, and Zoom, which may be selected by clicking on their icons.

The ***Selection*** tool (arrow) may be used to select geo-locations on the map by clicking or dragging to produce a selection box.

The ***Measurement*** tool (plus-sign) is used to measure distance and/or azimuth from north on the map. Drag from the reference point to the point of interest and distance and azimuth will be displayed in the readout strip above the map.

The ***Zoom*** tool (magnifying-glass) is used to switch to a map with a different scale factor. Clicking (the left button) with the Zoom tool on the ONC map will switch to the JOG map (4x zoom), and clicking on the JOG map will switch to the TLM map (5x zoom). Clicking the right button with the Zoom tool on a map will move to a map with the next lower zoom factor. Two additional zoom levels are available, with blank backgrounds. Zooming out from the ONC map produces a 4x zoom out (1:4,000,000 scale) to a blank background, and zooming in from the TLM map produces a 5x zoom in (1:10,000 scale) to a blank background.

4.1.4 Map Background

The ***Map*** popup menu to the left of the map provides a means of making the raster map background less obtrusive. The menu contains four choices: Color, B&W, Faded, and Blank. Color is the default choice and shows the map in its original colors. The B&W choice causes the map to be displayed in black and white. Faded is a whitened version of the black and white display. Blank eliminates the map background altogether.

The ***Overlays*** button provides a means of adding vector map features to the map background. They are plotted on top of the raster map, or if a Blank background has been selected, they are plotted on a white background. Figure 4-4 shows the dialog that is presented when the Overlays button is clicked. Features can be selected by clicking the checkboxes. The color used to plot each feature may be changed by clicking a Set Color button, which brings up a color dialog.

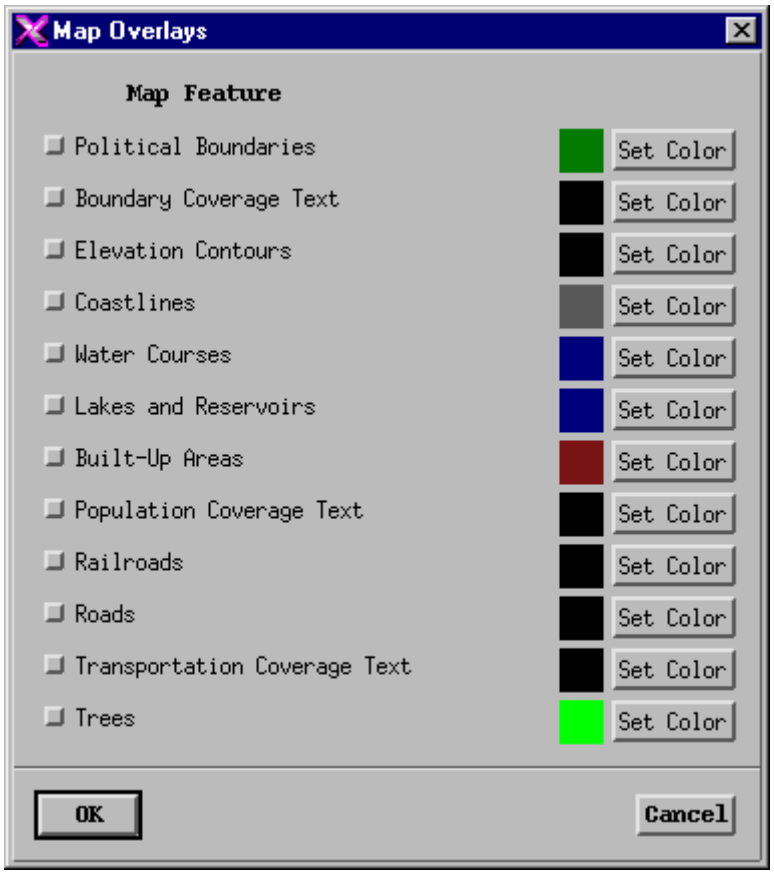

Figure 4-4. Map Overlays Dialog

4.1.5 Geolocation Reports

Geolocation reports, listed in the text field below the map, may be filtered, sorted, and selected. The ***Set Filter*** button brings up the Filter Dialog shown in Figure 4-5. Geolocation reports may be temporarily removed from the listing by setting ranges of values in the dialog.

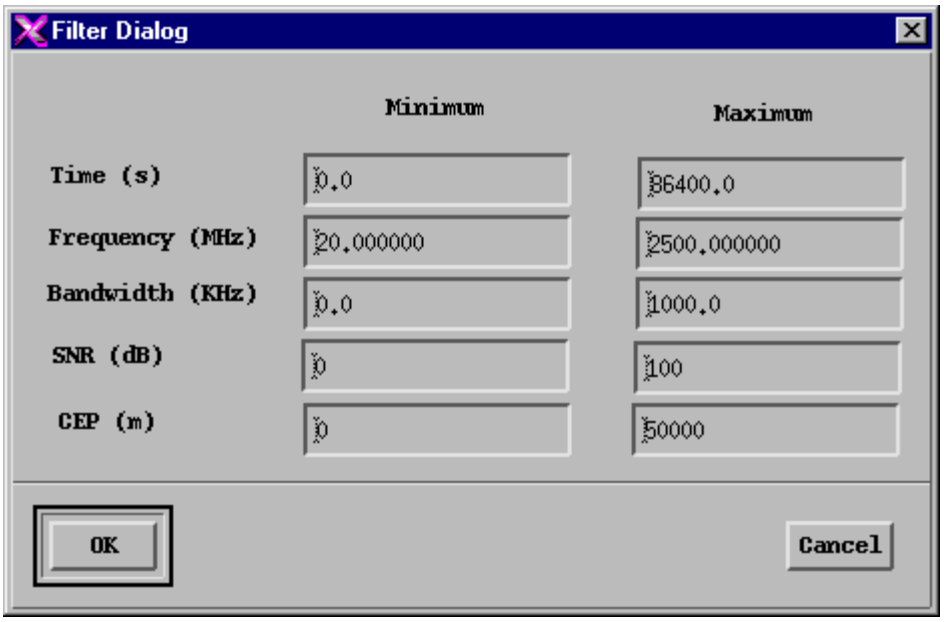

Figure 4-5. Filter Dialog

The ***List Selected*** button is used in conjunction with the ***Selection*** tool in the map window. After selecting geolocations on the map, clicking the ***List Selected*** button causes all non-selected reports to be temporarily removed from the listing and causes their error ellipses to be removed from the map. The ***Clear Filter*** button puts the temporarily removed reports back into the listing and plots their error ellipses on the map.

The ***Sort*** button brings up the Sort Dialog shown in Figure 5. The choices for the primary and secondary sort criteria are: Time, Frequency, Bandwidth, SNR, and CEP. After clicking ***OK***, the geo-location reports are arranged in the listing according to the selected criteria. The reports can be returned to their original order by clicking the ***Unsort*** button.

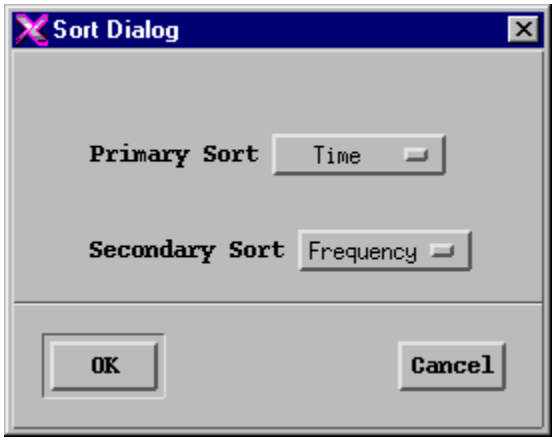

Figure 4-6. Sort Dialog

4.1.6 Platform Ground Track

The ground track for the collection platforms is plotted as the geolocation reports are plotted. The collection platform position is driven by a data file that defines an oval or racetrack shaped course in the standalone GeoDisplay-only demo.

4.1.7 File Interfaces

The files read by the geodisplay application include the geolocation reports file, collection platform trajectory file, master map file, which lists the map files for a given area, raster image map files, and vector map files. The geolocation reports file is a binary file of fixed length records that is intended to evolve with the PinPoint development. It currently contains time, latitude, longitude, semimajor axis, semiminor axis, CEP, velocity, heading, velocity CEP, frequency, bandwidth, SNR, modulation type, an indication of which platforms were involved in the geolocation and whether they measured TDOA, FDOA, or both; the platform names, and the file version number.

The collection platform trajectory file is a text file, whose first line is the keyword "Racetrack." The remaining lines each define a trajectory for a collection platform. The tab-separated columns consist of platform index, platform name, leg duration, turn duration, initial heading, initial speed, initial latitude, initial longitude, initial altitude, start date, and start time.

The master map file is a text file, whose first line is the keyword "Maps." Subsequent lines consist of three tab-separated columns containing an integer zoom level, the name of the raster image map file, and the name of a DTED file containing elevation data for the same area. Multiple lines may have the same zoom level; the map centered closest to the zoom click point will be displayed. This feature was implemented to improve the responsiveness of zoom operations by reducing the size of the map files, while maintaining a large area of coverage.

Raster image files have a format defined by the NIMAMUSE software, consisting of a header that defines the area covered by the map, and other parameters, followed by the raster image. The vector map files also employ a format defined by the NIMAMUSE software.

4.2 Simulated CAF/Geo Performance, Conventional Signals: Case 1

The results of a simulation run, carried out through the MatLab implementation, are given in the following sections to provide a concrete example of the expected typical Phase 2 geolocation performance. Two networks were modeled, one made up of relatively strong (~10 watts ERP) FM Voice emitters and the other with low-power (~1 watt ERP) FSK Data emitters. A single strong LPI interferor is modeled, along with four broadcast TV stations. Data was simulated for three platforms flying in a “Rocking K” formation about 40-100 km behind the forward edge of battle (FEBA), from which any two are selected for a geolocation analysis run. The operating frequency is 60 MHz, and the nominal duration of each transmission varies from 1 to 4 seconds.

For the purpose of comparing PinPoint to conventional geolocation, single-antenna CAF processing was also performed using the same PinPoint code, but using known SOI truth to cue the time-up, time-down, and initial geolocation cue-point for each transmission. The CAF peak

magnitude is thresholded for these cases, and the data is rejected if the CAF peak closest to the designated (SOI-truth) cue point is less than 12 dB above the median value over the entire unambiguous CAF surface. The single-antenna results are representative of the performance that would be obtained for these signals if a conventional geolocation system was cued with a co-channel detect-DF front-end.

4.2.1 Test Scenario Geometry, Case 1

The scenario geometry for this example run is illustrated in Figure 4-7, against a color-contour backdrop depicting the co-channel detection and 50% Circular-Error Probability (CEP-50) geolocation performance generated by the Phase 0 functional simulation code. The backdrop is computed for two-platform TDOA-FDOA against stationary conventional low-power (1 watt) emitters, using the widest platform baseline (platforms 1 and 3). The boundary of the color-contour region depicts the region over which both platforms detect and beamform the signal, which is required by the Phase 2 Demonstration System for real-time geolocations.

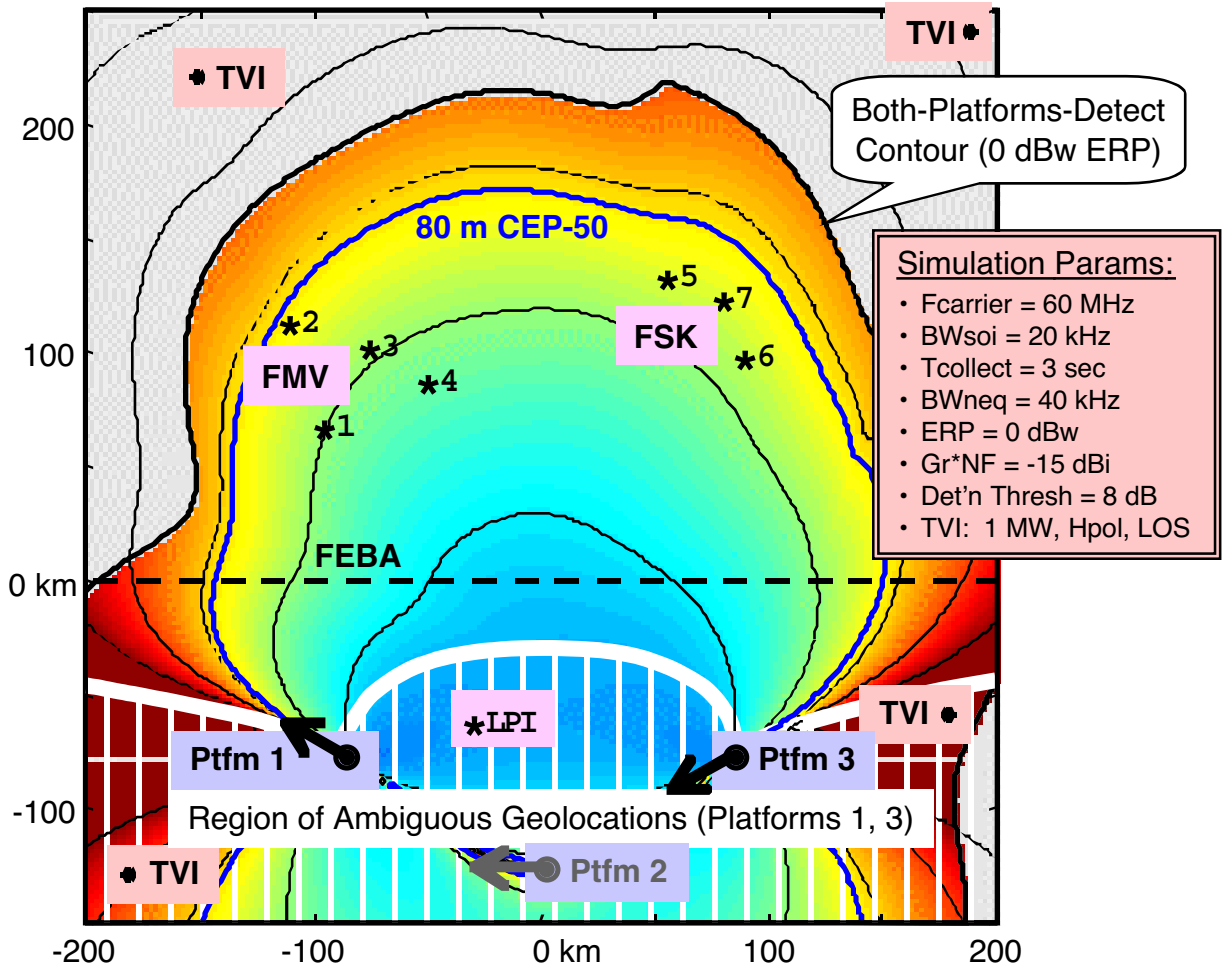

Figure 4-7. Simulation Scenario and Functional CEP-50 for Low-Power Emitter, Case 1.

A white-striped overlay depicts the region over which the TDOA-FDOA geolocation solution is ambiguous and would require DF cuing for resolution. The mapping from location to TDOA-FDOA is one-to-one (unambiguous) outside that region. Inside the region, each x-y point has an image point, also within the region, with the same TDOA-FDOA values. The target networks are well outside this ambiguity region, which is entirely behind the FEBA. As a result, DF cuing is not required for TDOA-FDOA geolocation of the nets. Instead, a single cue-point located roughly 100 km north of the FEBA center suffices for geolocation of all test emitters.

The simulation timeline for this example run is given in Figure 4-8, and consists of 30 seconds of data. The net transmissions are associated numerically with the emitters shown in Figure 4-7. Each net transmits five times, and the nets overlap (signal-on-signal) for three transmissions of each net. All but two of the transmissions experience LPI interference. The flight path of platform 2 is straight and level, while the paths of platforms 1 and 3 undergo turbulence (0.1 g rms on each axis, isotropic, 2 Hz rolloff) beginning at respectively 10 and 20 seconds into the run.

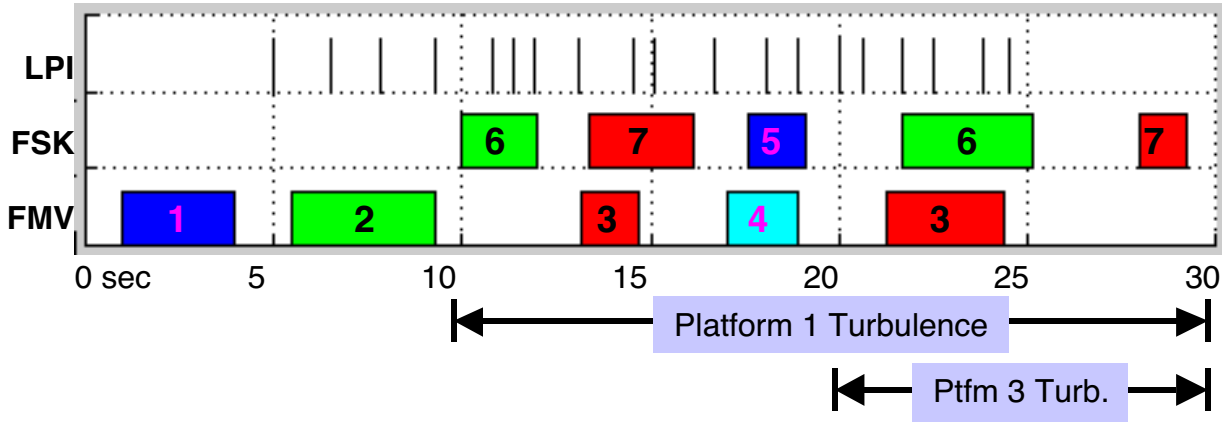

Figure 4-8. Simulation Emitter-Net Timing Diagram, Case 1.

4.2.2 Detect/Beamform Performance

The beamformer signal-up, signal-down detections and CMA port-lock statistics are plotted in Figure 4-9 for platform 1. Similar results are obtained for the other platforms. As seen in the figure, the beamformer locks stably onto each emission.

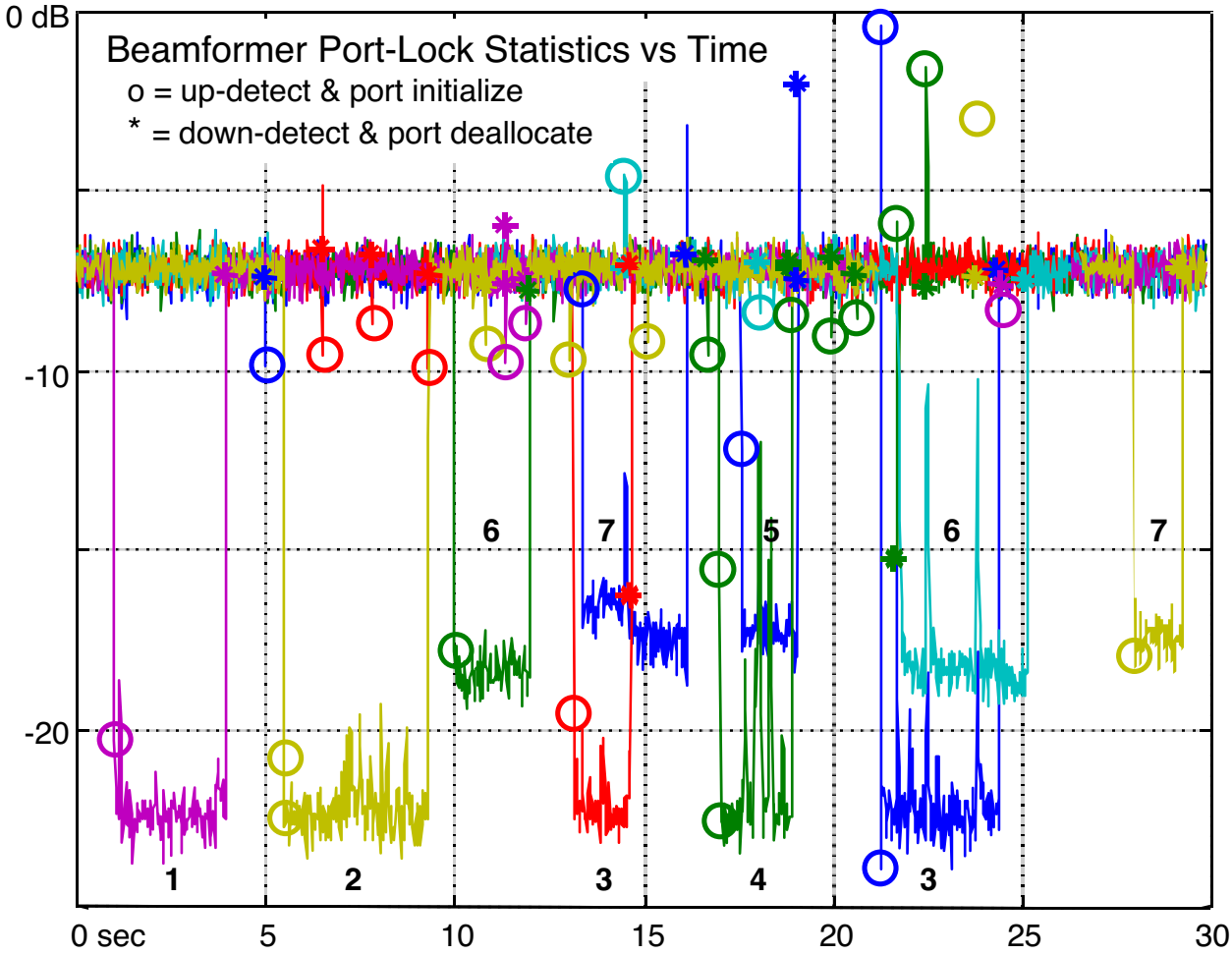

Figure 4-9. Port-Lock Statistics for Platform 1 Beamformer, Case 1.

The detectors currently implemented in the beamformer are optimized for operation as needed in a cued beamformer, to stabilize the weights in the presence of LPI and signal-on-signal, and to detect copy signal-down so that the beamformer can deallocate itself promptly to free up the associated receiver assets for another task. For the Phase 2 flight tests, these detectors are also performing the beamformer copy-tasking function, which in a fully operational SIGINT system would ordinarily be performed by a separate wideband detect/DF thread.

4.2.3 CAF/Geolocation With Beamforming

The full (unambiguous) motion-compensated CAF surface and geolocation error ellipse for one of the transmissions (Emitter Four, FM-Voice, from platforms 1 and 3) is shown in Figure 4-10, for the PinPoint (beamformer) CAF processing case. The locations of the emitters are translated into differential delay-Doppler and overlaid, along with a white rectangle depicting the stationary-target delay and Doppler maximum excursions for the platform positions and velocities at the time of the collect. (These quantities are computed on a location-by-location basis in order to automatically determine the required CAF block sizes for unambiguous, low-

loss integration.) The CAF surface is characteristic of a short-duration (2 second) collect of an FM Voice emission with no co-channel interference. The lack of discernable peaks in the locations of the TV interferors graphically demonstrates the beamformer nulling effectiveness.

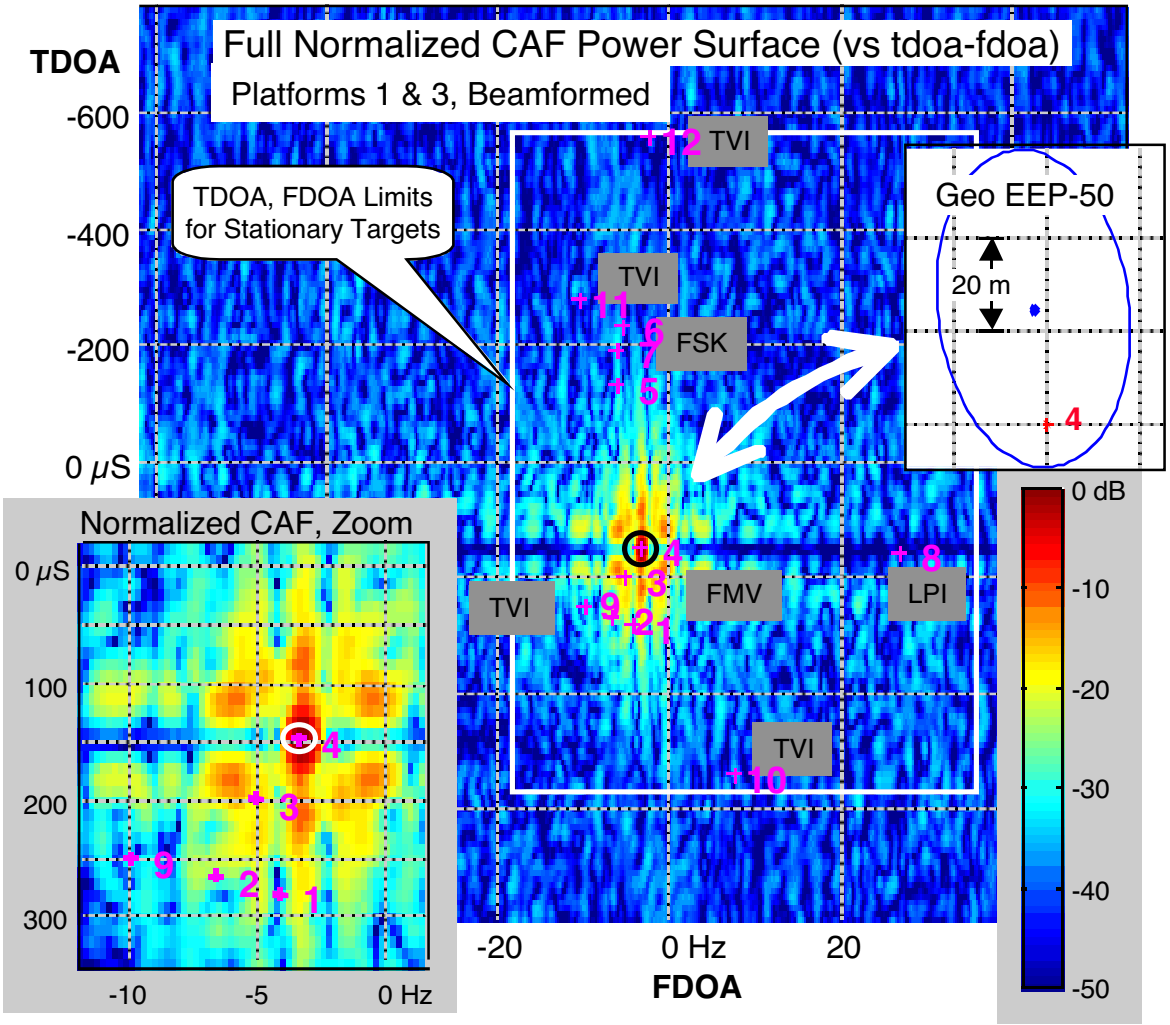

Figure 4-10. PinPoint CAF/Geo Performance at Emitter #4 (FM Voice), Platforms 1 and 3.

A zoom of the CAF peak at Emitter 4 is also shown. This zoom shows the CAF sidelobe structure typical of a two-second FM-Voice transmission. The normalized CAF peak power is nearly unity (zero dB), indicating a highly coherent motion compensated cross-correlation. In contrast, the background CAF noise level is roughly –40 dB (median value).

The geolocation solution and 50% error ellipse are shown relative to the SOI truth for Emitter 4 in the second overlay. The ellipse half-axes measure about 40 meters by 20 meters, for a CEP of roughly 30 meters. The error ellipse is determined by geometry and a combination of estimated values for TDOA and FDOA measurement errors, including engineering values for navigation, timing and reference stability error components as well as data-derived estimates based on collect duration, bandwidth and SINR.

4.2.4 CAF/Geolocation Without Beamforming

In contrast, the CAF surface and error ellipse for single-antenna CAF processing case with the same emitter, platforms, and simulation data set are shown in Figure 4-11. The two dominant CAF peaks on the surface are due to TV interferors (Emitters 10 and 12), and the CAF peak at the SOI (Emitter 4) is only slightly above the threshold (set at 12 dB above the CAF-median value, which was about -40 dB for this case). The sidelobe structure of the SOI is less evident only because the correlation peak is so much lower due to the effects of strong co-channel interference. The background CAF noise level is roughly –48 dB (median value).

The sidelobe structure of the TV interferors is more compact than would probably be encountered in a real collect, since the narrowbanded TV signal is modeled as a gaussian noise process that is blanked by 11 dB during the vertical retrace.

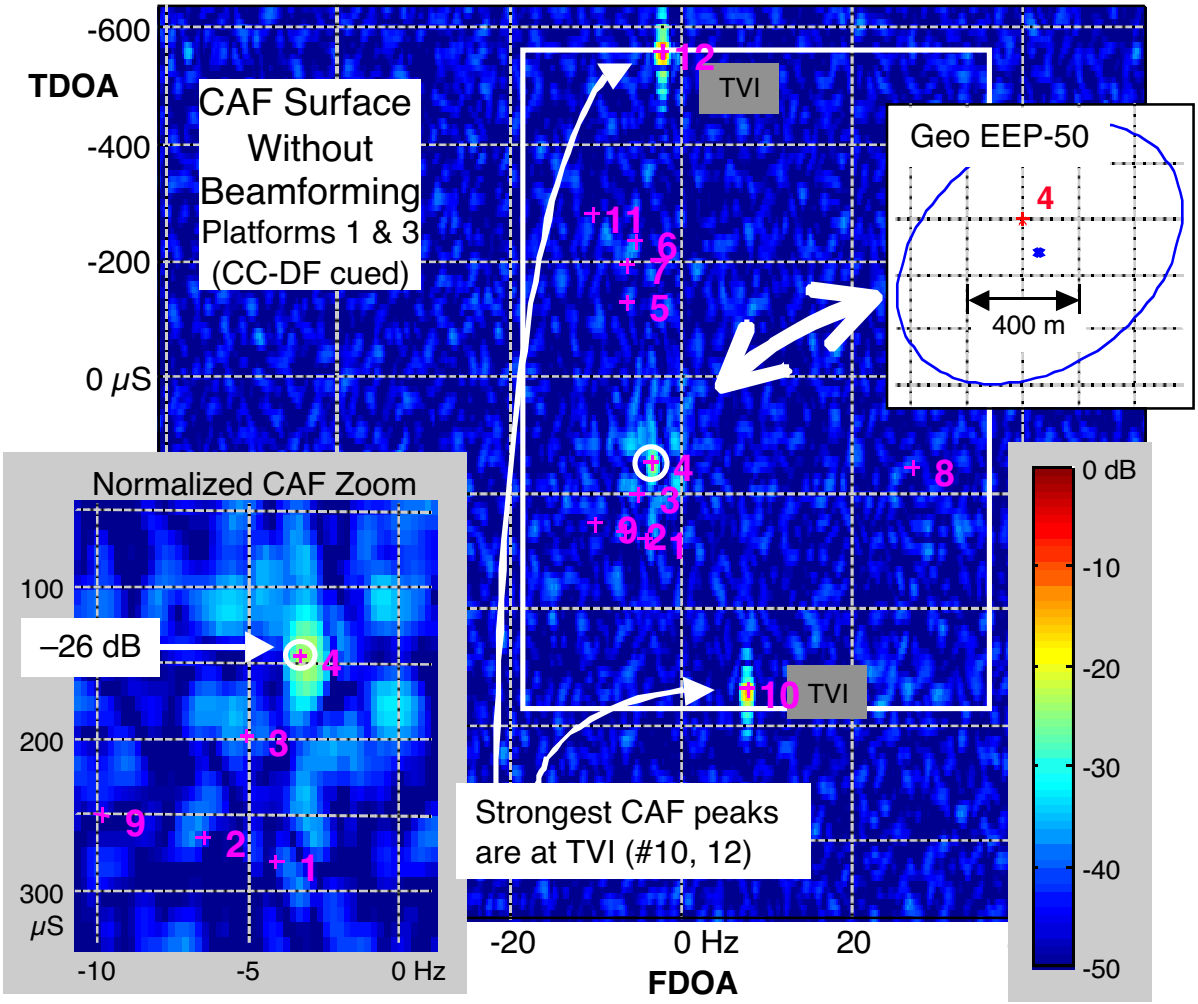

Figure 4-11. CAF/Geo at Emitter 4 Without Beamforming (Co-Channel Detect-DF Cued).

The location solution and estimated error ellipse are shown on the overlay. The estimated CEP is about 500-600 meters in this case, and the miss distance is much greater than that obtained with beamforming.

4.2.5 Compiled Geolocation Performance Results, Case 1

The geolocation results for the example simulation run, with and without beamforming, are summarized in Table 4-1. The minimum, median and maximum miss distances are given in meters for each pair of platforms and for each network over the 30 second simulation (five transmissions simulated per net). Geolocation with the "beamformer" CAF processing designation represents the PinPoint processing currently being implemented for Phase 2. Geolocation with the "single antenna" CAF processing designation represents geolocation without beamforming.

Table 4-1. Geolocation Accuracy Summary (meters), With and Without Beamforming, Case 1.

platforms	CAF processing	FM-Voice (strong emitters)			FSK (low-power emitters)		
		Min	Median	Max	Min	Median	Max
1 and 3	beamformer	20	63	123	33	89	99
1 and 3	single antenna	129	328	564	3040	-	-
2 and 3	beamformer	18	54	118	104	130	169
2 and 3	single antenna	911	2045	6040	5119	-	-
1 and 2	beamformer	23	91	141	68	82	91
1 and 2	single antenna	395	2104	4335	-	-	-

For the stronger (FM Voice) emitters, beamforming improves the geolocation results by a factor of 5 with platforms 1 and 3, and by factors of 20-40 with the other platform pairings. As shown in the table, the low-power emitters require beamforming for geolocation. These transmissions are generally too short to generate enough integrated SINR to obtain a valid CAF peak.

Finally, comparing the median results of Table 4-1 to the (Phase-0 functional simulation) predicted results given in the Scenario Overlay of Figure 4-7, for platforms 1 and 3 with the low-power emitters, the performance achieved by the high-fidelity data-driven simulation are seen to be in very close agreement with those predicted by the functional simulation. This agreement provides a point of validation of the Phase 0 performance prediction analyses.

4.3 Simulated CAF/Geo Performance, Conventional Signals: Case 2

Another test case was simulated for a very similar geometry, the main differences being the removal of the LPI interferor and addition of an AM emitter. The results are summarized in this subsection, and include a more detailed analysis of the nature of the errors for the non-beamforming case, as well as the beamforming case both with and without the use of the Radix Proprietary beamformer stabilization technique.

4.3.1 Test Scenario Geometry, Case 2

The test geometry for Case 2 is shown in Figure 4-12. The low-power closely spaced FSK-data net consists of four members, the vehicular FM-Voice net only two members, and a single AM Voice emitter is included also to illustrate the beamformer performance on standard (unsuppressed carrier) AM Voice. The platform and television interference (TVI) geometry is the same as that for Case 1. The array geometry shown in this figure was also used for Case 1.

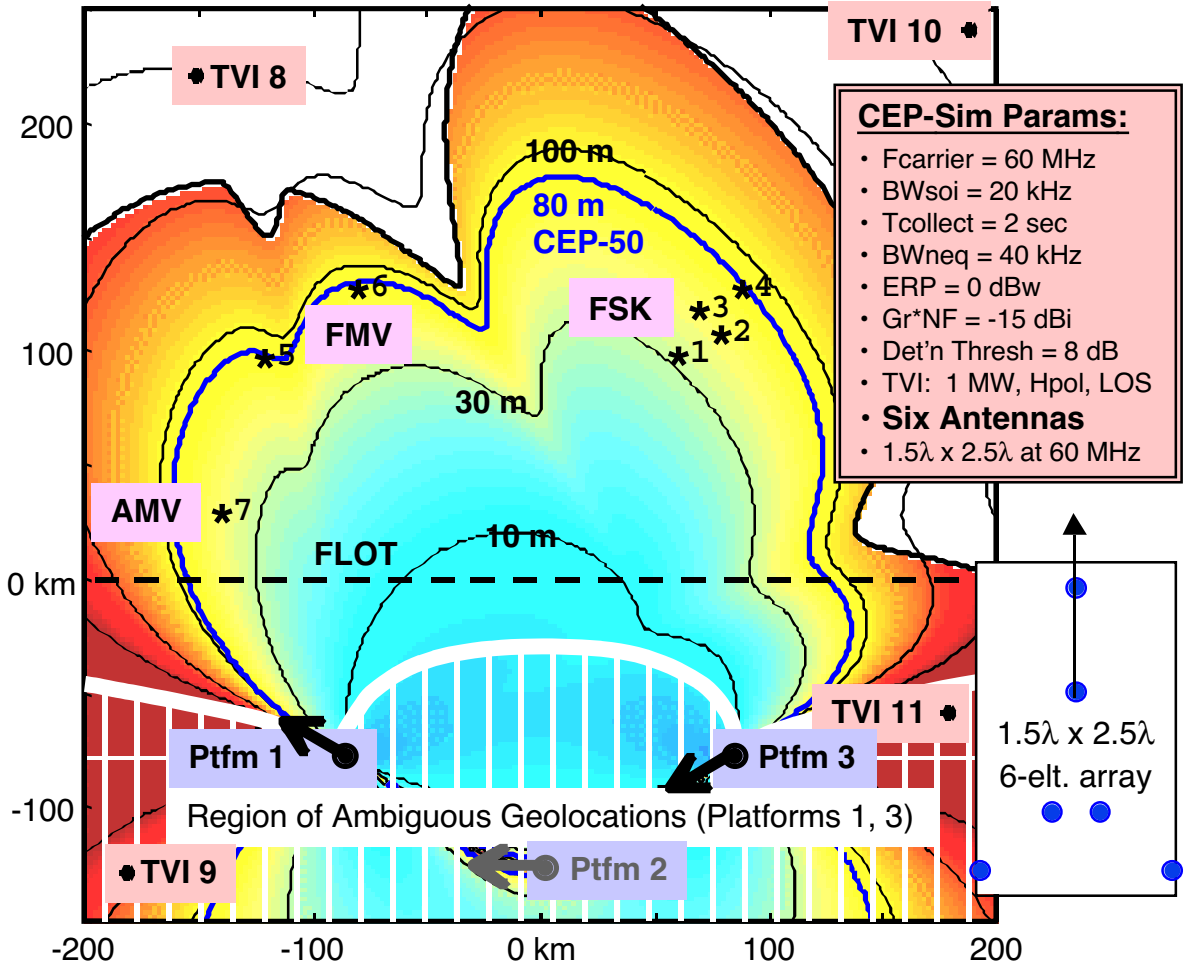

Figure 4-12. Simulation Scenario and Functional CEP-50 for Low-Power Emitter, Case 2.

The television and tactical emitter power levels used in the simulation are given in Table 4-2. The table includes the approximate effective radiated power (ERP) for each of the tactical nets that would result in the stated power levels at the platforms according to the propagation loss models used in the Phase 0 functional CEP calculations. The TVI power levels have been varied substantially from the Phase 0 model, in order to simulate the effects of variations in TV power spectral density from the average values used in Phase 0.

Table 4-2. TVI and Emitter SWNR at Antennas, Case 2.

TVI #	SWNR@antenna, dB:			Net	~ERP,	SWNR@antenna, dB:		
	Ptfm 1	Ptfm 2	Ptfm 3	type	dBw	Ptfm 1	Ptfm 2	Ptfm 3
8	20	10	10	AMV	+3	25	20	20
9	40	40	30	FMV	+10	20	20	20
10	10	20	20	FSK	–3	10	10	15
11	30	30	40					

The emitter net timing is shown in Figure 4-13. The simulation duration is 10 seconds, during which we have 5 transmissions from the FSK net, and 3 transmissions from the voice emitters. This level of signal activity is quite high for a single narrowband channel, and the transmissions are shorter than would ordinarily be expected, in order to pack a lot of geolocation activity into a short simulation run. On the average, about 1.5 tactical signals are up at once, and every emission displays at least some signal-on-signal (not counting the steady state TV interference background).

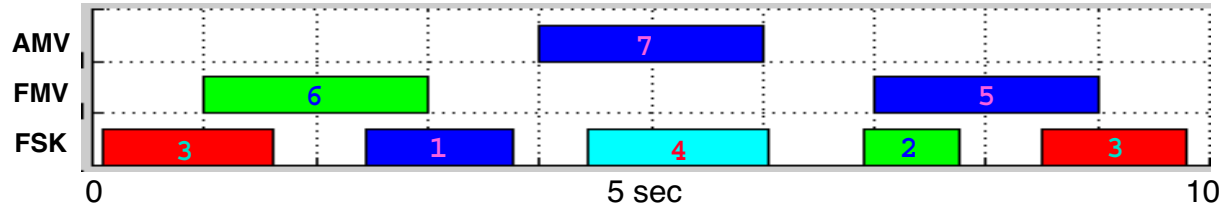

Figure 4-13. Simulation Emitter-Net Timing Diagram, Case 2.

The co-channel environment dynamics are illustrated in Figure 4-14. The eigenvalues of the six-antenna sample covariance matrix for each 20 mS adaptation block at platform one are plotted versus time. These eigenvalues are best interpreted as the co-channel residual noise floor after steering respectively zero, one, two, etc. nulls.

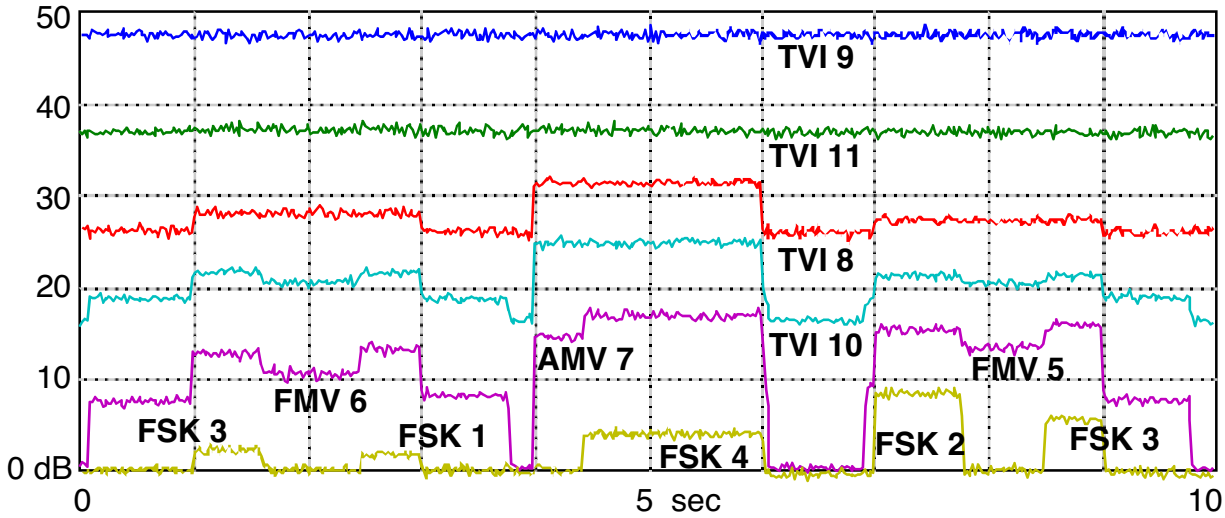

Figure 4-14. Co-Channel Environment (Covariance Eigenvalues) for Platform 1, Case 2.

Without any nulls, the strongest TV station (TVI 9) dominates the environment. With two nulls on the strongest two TV stations, activity is just discernable for the strongest tactical signals. All six antennas are needed to null the four TV signals and separate two overlapping tactical signals.

4.3.2 Compiled Geolocation Performance Results, Case 2

The co-channel processing detects and beamforms all eight of the tactical emissions at each of the three platforms, and geolocation is therefore properly cued for each emission between any pair of the three test platforms. The detailed geolocation results for platforms one and three are given in Table 4-3, for the cases of full PinPoint beamformed geolocation ("bf stab"), beamformed geolocation without using the Radix-proprietary stabilizer techniques ("bf only"), and single-antenna (per platform) geolocation cued by co-channel detection and (zero-error) DF ("no bf").

Table 4-3. Geolocation Performance Summary (meters), With and Without Beamforming and Stabilization, Platforms 1 and 3, Case 2.

emitter	3	6	1	7	4	2	5	3
time up	0.10	1.00	2.46	4.00	4.44	6.90	7.00	8.50
time dn	1.60	3.00	3.76	6.00	6.04	7.76	9.00	9.78
geo_miss_m:								
bf stab	71	108	34	64	103	30	121	77
bf only	62	56	219	324	536	437	196	300
no bf	NaN	866	NaN	7168	NaN	NaN	1452	NaN
geo_Pscore:								
bf stab	0.243	0.053	0.698	0.358	0.235	0.873	0.052	0.194
bf only	0.312	0.419	0.000	0.000	0.000	0.000	0.000	0.000
no bf	NaN	0.690	NaN	0.074	NaN	NaN	0.515	NaN
tdoa_miss_nS:								
bf stab	52	-42	10	-50	-35	18	10	64
bf only	51	-42	3	-53	-34	19	8	67
no bf	NaN	379	NaN	14155	NaN	NaN	-2795	NaN
fdoa_miss_mHz:								
bf stab	-4	-5	-2	-3	-4	-2	-5	-4
bf only	-3	-3	15	-15	-24	-24	-9	-16
no bf	NaN	-39	NaN	-15	NaN	NaN	-41	NaN

First, the miss distances for each technique are given in meters ("geo_miss_m"). In nearly every case, the stabilized beamfoming greatly outperforms unstabilized beamforming. The non-beamformed geolocation cannot even detect a correlation peak for the low-power FSK emitters, and yields kilometers of error with the stronger tactical signals (FM, AM Voice).

The error statistics are reasonably bias-free for the stabilized beamformer and non-beamformed cases, as indicated by the corresponding P-scores ("geo_Pscore"). The P-score is the probability

that the X,Y location would have a greater elliptical error (lie on a larger scaled-error-ellipse) than it does. The high P-scores seen for the PinPoint (stabilized beamformer) cases, as well as the non-beamformed cases that yield measurements, indicate that the true locations fall within the estimated 95% error ellipses about the measured locations. In contrast, the very low P-scores displayed for the beamformer case without stabilization are indicative of a substantial measurement bias.

The miss errors in TDOA ("tdoa_miss_nS") for each case are given in nanoseconds, and the FDOA errors ("fdoa_miss_mHz") are given in milliHertz. The TDOA errors are roughly the same for the two beamformed cases (with and without stabilization), as would be expected for fixed-frequency beamforming. The unstabilized beamformer location errors instead derive from FDOA errors that arise due to the inherent phase ambiguity of a typical adaptive beamformer. In contrast, the FDOA errors are relatively small for the non-beamformed case, and the geolocation error is primarily due to large TDOA errors as would be expected for narrowband, low-SINR collects.

The geolocation miss distances are given for each platform pair, and for all three beamforming cases (beamforming with and without stabilization, and without beamforming) in Table 4-4. The relative performance is similar between each pair of platforms.

Table 4-4. Geolocation Accuracy Summary (meters), With and Without Beamforming and Stabilization, All Platform Pairs, Case 2.

emitter	3	6	1	7	4	2	5	3
time up	0.10	1.00	2.46	4.00	4.44	6.90	7.00	8.50
time dn	1.60	3.00	3.76	6.00	6.04	7.76	9.00	9.78
geo_miss_m, Platforms 1 & 3:								
bf stab	71	108	34	64	103	30	121	77
bf only	62	56	219	324	536	437	196	300
no bf	NaN	866	NaN	7168	NaN	NaN	1452	NaN
geo_miss_m, Platforms 2 & 3:								
bf stab	69	103	22	69	149	72	106	94
bf only	315	278	227	78	1389	558	165	85
no bf	NaN	10499	NaN	3036	12262	NaN	1978	NaN
geo_miss_m, Platforms 1 & 2:								
bf stab	59	124	47	148	77	7	152	95
bf only	197	180	707	764	202	375	250	561
no bf	NaN	NaN	NaN	22011	23967	NaN	NaN	NaN

Over all of the locations in Case 2, the PinPoint (stabilized beamformer) performance yields a median miss distance of 77 meters. Beamformed geolocation without stabilization yields a substantially degraded median miss distance of 265 meters. These results show that the stabilizer dramatically improves performance; by a factor of three overall, in this case.

Without beamforming, only the strong signals yield discernable CAF peaks in nearly all cases, and the median miss distance is 7.2 kilometers. In fact, the CAF threshold of 12 dB above the median floor is probably too high and admitted a few false detections. If we cull the worst locations from the results (presumably achievable by raising the CAF detection threshold some) then we could reduce the median miss distance to 2.5 kilometers, with a probability of successful geolocation of about 2/3, for the strong tactical emitters. In any case, these results clearly indicate that even unstabilized beamforming is much better than no beamforming at all.

5. PinPoint Program Migration Plan

The overall PinPoint migration plan as currently envisioned is to move rapidly at the completion of the Phase 1 contract to a Phase 2 flight demonstration program to prove with real data the advantages of precision beamformed TDOA-DD emitter location processing. The optimal Phase 1 hardware choices are dependent upon the scope of the Phase 2 flight demonstration and subsequent anticipated Pinpoint development phases. This discussion is notional and is intended to provide a baseline for discussion and solicitation of Government comments, directions and recommendations for the overall PinPoint program plan.

5.1 Migration Plan Overview.

A candidate Migration Plan schedule is shown as a timeline in Figure 5-1. To minimize Phase 2 costs, Radix is recommending a limited system configuration to validate the emitter location precision of the Pinpoint, perhaps in conjunction with flight testing of the Nonlinear Resonance Classification (NRC) function using a beamformer front-end, depending on the program plan and priorities of the ongoing Radix-Army NRC effort. The envisioned Phase 2 system will process a single frequency channel (narrowband) to geolocate emissions from conventional push-to-talk radios operating in a simplex net on a pre-arranged frequency. A much more complete SIGINT system functionality is envisioned for Phases 3 and beyond, including scanning signal search for conventional co-channel detect/DF with drop-receiver cueing and/or extended dwell capability for geolocation, and staring LPI signal processing for co-channel detect, DF, track, and geolocation. Final Pinpoint migration to a host system would not occur until Pinpoint Phase 4.

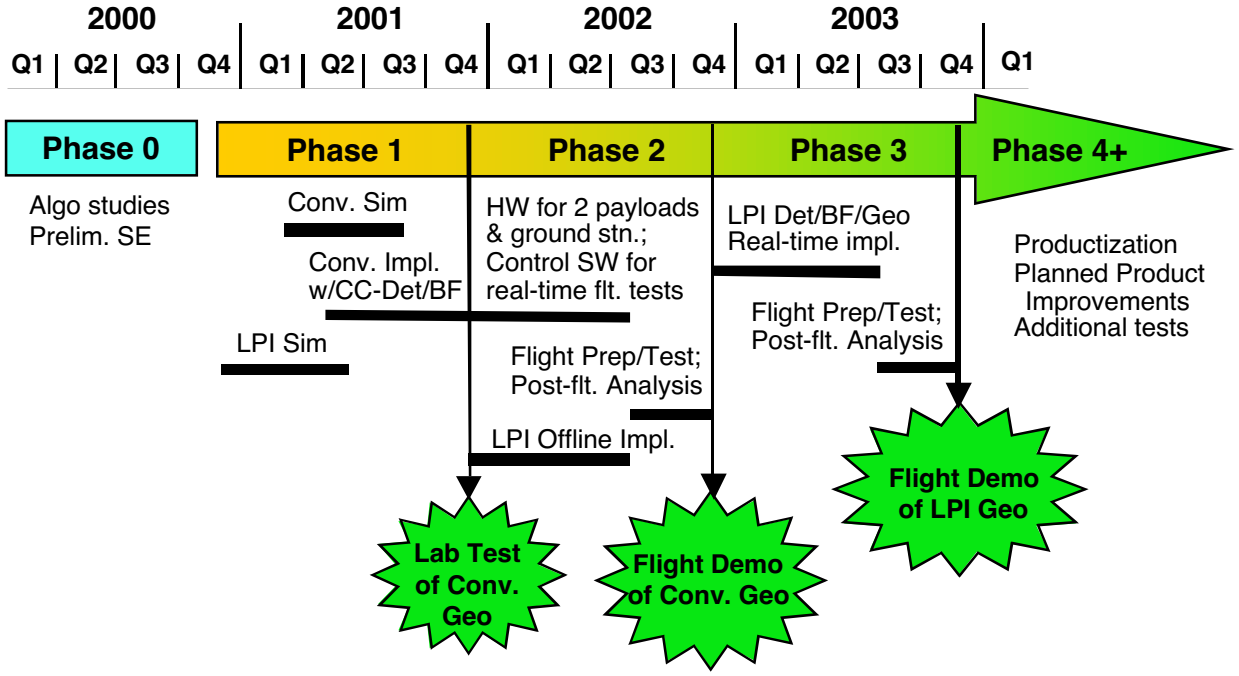

Figure 5-1. Notional PinPoint Migration Plan Schedule

As a baseline for Pinpoint flight test planning, we assume that we will use the two CECOM Guardrail aircraft and the associated ground Integrated Processing Facility (IPF) located in New Jersey. Since these aircraft are configured with older generation Guardrail payloads that do not support beamformer processing, either wideband or narrowband, the flight tests will require the introduction of multi-channel receivers and other hardware on each aircraft. This hardware is beyond the scope of the Phase 1 hardware purchase which is targeted only at the PinPoint processing element, but the configuration and migration plan does impact the optimal Phase 1 hardware selection. With careful planning we can assure hardware and software acquired for each phase migrates forward efficiently.

We are recommending the purchase of COTS receivers and other hardware that will be flown on the two Guardrail test aircraft early in Phase 2, in support of Pinpoint phases 2 and 3. Radix has carefully investigated COTS equipment in support of our CECOM DTSP proposal and found that good quality equipment is commercially available that can also support Pinpoint flight testing.

The current PinPoint migration hardware concept employs Eclipse VME tuners covering the 30-1000 MHz band, Ixthos VME Quad-G4 DSP cards with Raceway++ interconnects for the signal processing, and a Sun workstation for the ground station and HMI.

5.2 PinPoint System Requirements

Pinpoint system requirements are similar to those of traditional multi-platform Time Difference of Arrival-Differential Doppler TDOA-DD emitter location systems, in conjuction with those of traditional airborne multi-channel DF systems.

5.2.1 System Navigation, Timing and Coherence Requirements

To provide accurate signal location estimates, we must accurately know the location coordinates of the platforms and the precise times the signal data is collected. This is the case whether the sensor payloads are supporting TDOA-DD or AOA DF emitter location processing. Differential doppler measurements require knowledge of the velocity vector (speed and heading) for each platform as well as a highly precise frequency reference for the receiver local oscillator. Pinpoint does not have any particular navigation, timing or coherence accuracy requirements beyond those of any other TDOA-DD system.

The LBSS system employs precision GPS-disciplined INS and Rb standards for extremely high short-term platform Nav accuracy (position, velocity errors are small and roughly constant with time over periods of several seconds) and extremely stable frequency measurement accuracy. Phase 0 analyses have shown that this level of precision supports accuracies well in excess of the Army precision-targeting requirements in favorable geometries, and even at modest ranges with a standoff geometry.

The Phase 2 and 3 flight test instrumentation will likely be taking a step down in instrumentation precision from LBSS. We currently plan on using a commercial vector-GPS navigation system with an oven-controlled crystal oscillator (OCXO) reference. Recent internal studies indicate these less-precise instruments still support precision-targeting levels of accuracy, with little

degradation relative to the LBSS instrumentation at the longer ranges and less favorable standoff geometries. The limitations in accuracy become more evident only at the shorter ranges.

5.2.2 Receiver TDOA Compensation Requirements

Special compensation hardware and software is required to remove the receiver group delay differences between receivers or receiver channels in the multiple platforms. The receiver group delay must be measured at each platform by injecting a calibration RF signal at the front-end of each receiver that is precisely modulated with a BPSK code locked to the system clock. This code is used as a paradigm for correlation by the compensation software, to obtain an exact, phase-coherent measurement of the receiver channel frequency response, from which the group delay can be derived. This is a dynamic calibration process that compensates for group delay changes caused by receiver temperature and receiver gain settings. For Pinpoint, multiple receiver channels are used that must all have group delay compensation. Depending on the accuracy required, TDOA compensation can be as simple as taking the average group-delay across the receivers in each platform, or may require a more exact computation of the beamformer frequency response to derive the effective group delay on the signal of interest.

5.2.3 A/D Timing and Frequency Stability Requirements

The system A/D sampling clock (ADC) is phase-locked to the master oscillator (OCXO) which is in turn locked to the GPS 1-PPS timing marker. The individual samples must be referenced unambiguously back to GPS time either through a data packeting synchronization step or, as a minimum, a synchronous sample counter that is reset at 1-PPS markers along with a capability to read out the current 1-PPS epoch time. The Eclipse receivers being evaluated for Phase 2 provide both time-tagging of A/D data packets with epoch time and sample count data in the packet headers, and a highly convenient receiver synchronization function that causes the A/D data from receivers in a bank to be aligned in the corresponding data packets.

The short-term frequency stability of the OCXO master oscillator employed in the Eclipse tuners is expected to be sufficient to support PinPoint FDOA geolocation accuracy requirements when phase-locked to the GPS 1-PPS marker. Informal conversations with Eclipse indicate the stability is on the order of 1e-11 or so on the bench, which supports FDOA measurements of mHz accuracy through the tactical VHF band, which is more than adequate for PinPoint requirements. Since the crystals are temperature-controlled in ovens, the dominant source of frequency instability on an airborne platform would probably be vibration. More analysis (and data) would be required to assess this source of instability.

5.2.4 Pinpoint Unique System Requirements

There are some requirements that are unique to the PinPoint system, that address interactions between TDOA-FDOA measurement and co-channel beamforming. These requirements are primarily algorithmic in nature.

5.2.4.1 Beamformer Phase Compensation

The beamformer weight adaptation algorithms generally have an inherent phase ambiguity that can modulate the output waveform with respect to the actual received waveform over time. The effects can vary from imposition of a low-frequency doppler offset on conventional-signal collects to complete decoherence over even modest time intervals on LPI collects. For LPI signals, the long-term coherent processing required for PinPoint precision geolocation is achieved through beamformer phase stabilization with the aid of a conventional DF array calibration table. For conventional signals, a similar stabilization can be employed, or alternatively a blind stabilization technique can be applied provided the signal angle of arrival does not change appreciably over the duration of the collect. The latter approach is proposed for PinPoint Phase 2, in order to avoid the cost and schedule associated with the collection of DF array calibration tables and their integration into the system.

5.2.4.2 Beamformer Paradigms

Under some signal conditions only one of the platform sensors will be able to detect and beamform a signal-of-interest (SOI). In this case, beamformer data from the sensor that detects the signal can be used to aid in steering the beamformers in the other sensors. The data link loading is minimized by sending the beamformer paradigm to the sensor that does not detect the signal, and to perform paradigm-aided beamforming and CAF processing in that sensor. An alternative approach that is particularly attractive in the near-term, is to cue a multi-antenna, narrowband collect from that sensor and to perform the paradigm-aided beamforming for that sensor on the ground. Besides data link loading, the cuing time latency and memory buffer requirements for the implementation must also be considered.

5.2.4.3 Special LPI Related Signal Processing Requirements

LPI adds special requirements to the Pinpoint signal processing to detect and track the emissions, and to provide the wideband data buffering required for look-back beamforming. Paradigm beamforming for cases where only one platform detects the signal requires substantial cross-platform cuing coordination and/or deep wideband memory buffering. Many of these functions are required for LPI processing independently of PinPoint, and may become available for use by the PinPoint program in time for Phase 3. For this reason, LPI processing is being deferred to beyond Phase 2, since otherwise these functions would have to be developed at least in part by the PinPoint program.

5.3 Phase 2 Demonstration System

A block diagram of the Phase 2 Demonstration System is shown in Figure 5-2. The system consists of two airborne payloads, or Air Elements, and a ground station, or Ground Element. Each Air Element payload will be built up from COTS VME/RaceWay receivers and DSP cards hosted in a VME chassis with RaceWay backplane, and the ground station will be a Sun Sparc 5 workstation. The payloads and ground station communicate through standard Ethernet interfaces using standard TCP-IP and/or FTP networking protocols.

The airborne payloads will perform continuous, real-time co-channel beamforming on a designated narrowband channel, with integrated signal-up and signal-down detection for the cuing of geolocation processing. The geolocation processing is "pushed" by signal detections on the payloads, and the locations are displayed on the map as the test emitters transmit, for a real-time display of emitter activity. The payloads will also support both wideband and narrowband multi-antenna snapshot collection and download, TDOA compensation data collection and download, and implementation of TDOA compensation filtering using FIR filter weights uplinked from the ground workstation.

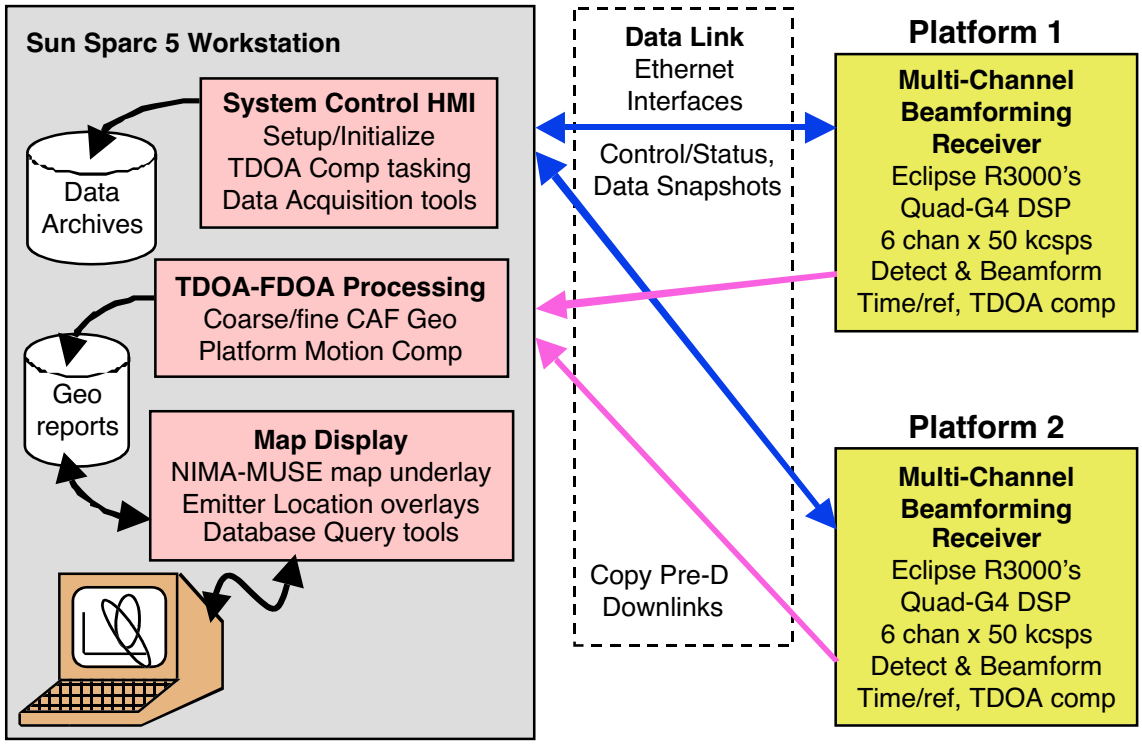

Figure 5-2. PinPoint Phase 2 Demonstration System Block Diagram.

The ground station will control the payloads, perform the inter-platform data correlation (motion-compensated CAF) and geolocation processing, and display the locations with estimated error ellipses on a map. Additionally, the ground station will be able to task snapshot collections, perform analyses to quantify the co-channel environment and/or validate the snapshot collects, and to task and process TDOA compensation collects.

The GFE datalink interfaces are assumed to be Ethernet-compatible, and the link capacity is assumed to fully support at least one 10-base-T bidirectional connection between the ground station and each payload. The downlink data rate required for real-time geolocation could be quite modest, as it depends primarily on the scripting of the test emitter timelines, but higher rates would be very helpful to support timely data snapshot downloads. The uplink rate required is much less for Phase 2, since only command and control messages are sent up the link. For Phase 3 and beyond, however, greater uplink bandwidths may be required to support paradigm uplinks for on-board geolocation tests and/or paradigm-aided beamforming.

5.3.1 Air Element Architecture

The Air Element hardware consists of 6U-VME receivers and DSP cards hosted in a VME chassis with a RaceWay backplane. The hardware configuration for Phase 2 is shown in Figure 5-3. Three Eclipse R3000 dual receiver cards (or equivalent) are proposed, with both channels configured for 20-1000 MHz operation to provide a six-channel coherent receiver. The local oscillators and A/D sample clocks are phase-locked to a common reference and stabilized relative to GPS time, with absolute timing resolution of 25 nS and frequency stability on the order of 10^{-11}, via the Eclipse Ref-1000 module (or equivalent).

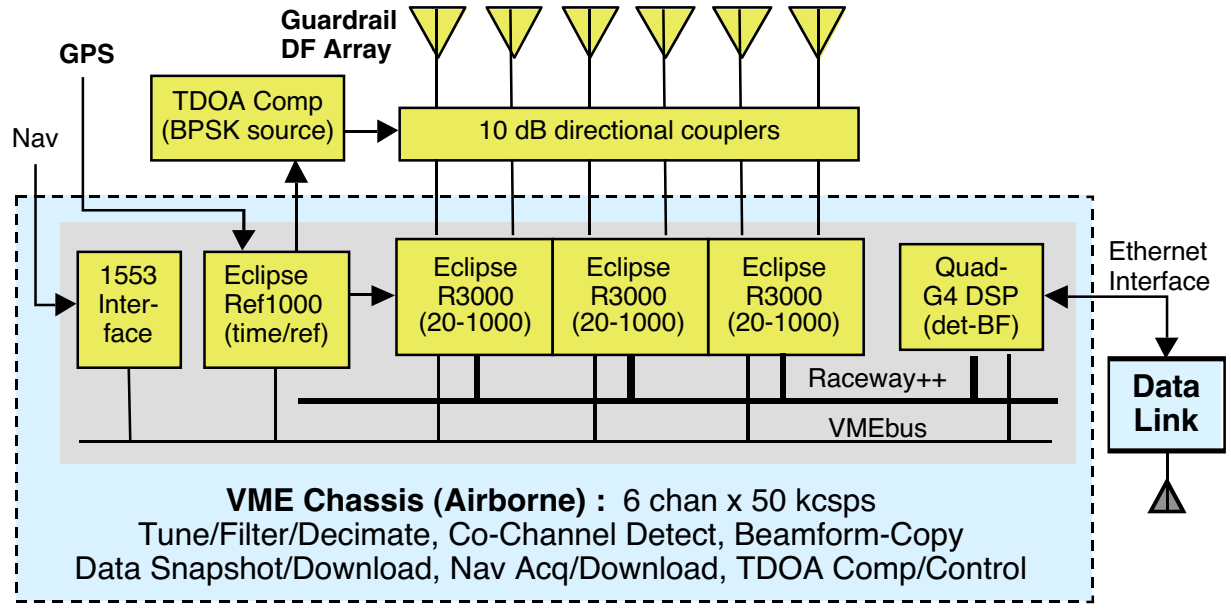

Figure 5-3. Phase 2 Flight Demonstration System, Air Element Hardware.

The Eclipse tuners digitize an instantaneous bandwidth of 15 MHz with a spur-free dynamic range of 75 dB. Each channel also carries a bank of 32 narrowband digital downconverters (DDC's), which are independently controlled and whose outputs are independently Raceway-addressable. The DDC's are synchronizable across channels, and will be used for the computationally intensive tune-filter-decimate function to provide a nominally 40 kHz narrowband channel sampled at 50 kHz complex.

The absolute group delay of each receiver is measured by injecting a precisely modulated BPSK waveform into the front-end, with directional couplers as shown in Figure 5-3. Laboratory COTS equipment (Radix, GFE, or rental) may be used if sufficient modulation synchronization and accuracy can be supported. Otherwise, a custom VME card will be designed and built.

A single Ixthos Quad-G4 card is located in VME Slot 0, and provides the beamforming DSP and data snapshot buffering functions. Through its on-card G3 controller, this card also controls the VME backplane and provides the Ethernet interface to the data link. Finally, a 1553 interface card is used to acquire the platform navigation data.

The Air Element payloads are highly modular and reconfigurable, and are readily expanded and upgraded with upward-compatible DSP and receivers. The same general architecture supports PinPoint Phase 3 and beyond, through the addition of DSP cards and perhaps also more receiver cards if required. The architecture readily supports development and demonstration of a wide variety of SIGINT functionality, and can be reused on many other future Army development programs as well as PinPoint.

A functional block diagram of the Air Element signal processing and control code hosted on the Ixthos Quad-G4 card is shown in Figure 5-4. The narrowband tuner data is received as a continuous stream of time-tagged Raceway packets from the Eclipse tuner DDC outputs. The channel group delays are equalized to a common reference delay via FIR filters on the G4 DSP(s). The equalized data is processed by the Beamformer Module, which both detects signals and generates beamformed copy snapshots of each detected signal. Navigation data is continuously forwarded out the data link regardless of the extent of signal activity.

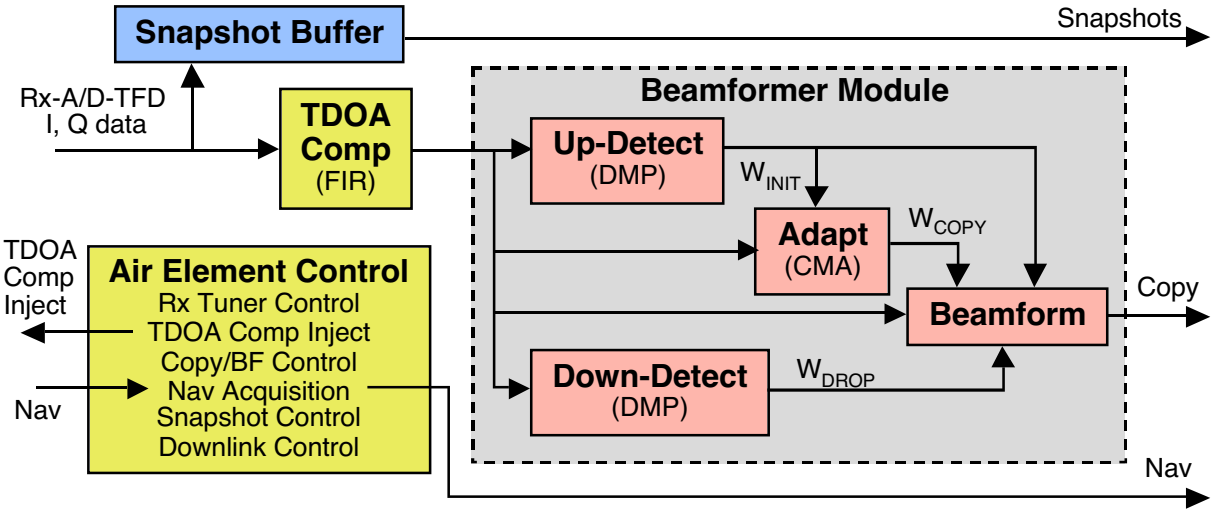

Figure 5-4. Phase 2 Flight Demonstration System, Air Element Functional Diagram.

The beamformer module segments the contiguous data into blocks (nominally 5-20 mS, operator-controlled) and adapts a bank of beamformers over each block using decimated data. The baseline adaptation process is the Multi-Target CMA algorithm, whereby the beamformers are adapted to minimize the modulus variation at the output of each beamformer while maintaining some degree of orthogonality between the beamformers to prevent them from all converging to a single signal. The adapted weights for a subset of those beamformers are then applied to the undecimated data to generate copy data for the designated beamformers.

A co-channel new-energy detector (DMP) is used to detect the onset of a signal by comparing the data covariance statistics across successive data blocks. When a signal-up is detected, a beamformer is assigned to the new signal, and the new beamformer is designated for copy generation associated with that report.

The same co-channel detector is used in reverse-time to detect a signal-down in the current data block. If the signal-down is positively associated with a copy-designated beamformer, copy is terminated and a signal-down report for that copy task is generated.

Finally, copy tasks are terminated after some timeout period (nominally 2-4 sec) to close off the signal report and initiate geolocation processing, whether a signal-down was detected or not. The CMA beamformer will still continue tracking the signal for as long as it stays up, but copy data will not be generated and passed down the link after the initial geolocation data is captured.

The TDOA compensation waveform generator is controlled by the G3 Controller processor on the DSP card, in accordance to commands from the Ground Element. TDOA compensation data is collected and passed down the link either periodically or on operator command. The compensation FIR filter weights are then calculated in the Ground Element and passed back up the link to update the TDOA compensation filters.

A narrowband snapshot mode will be provided, wherein the DDC outputs are buffered on the Ixthos quad-G4 card for the desired collect interval and passed down the link at the nominal link rate. The maximum collect duration is dependent on the operator-defined bandwidth and Ixthos memory limitations. We expect to support collect durations of up to 50 seconds at 50 kcsps (35 kHz bandwidth) by six antennas.

A full-bandwidth snapshot mode will also be provided, using the Eclipse delay-memory buffers. For this mode, the raw A/D samples (40 Msps, 16 bit real) are buffered and downloaded at the nominal link rate for the desired number of receivers. The maximum collect time for this mode is approximately 1 second, as determined by the depth of the Eclipse delay memory.

Narrowband snapshot collects will be collected to support algorithm development and offline demonstration of additional PinPoint beamforming approaches, such as paradigm-aided beamforming and CAF processing, which addresses cases where one platform detects and beamforms a signal but the other platform does not. Narrowband collects will also be useful for testing general multi-antenna, multi-platform CAF processing techniques that address cases where a signal is detected but, due to its modulation statistics, cannot be copied with blind-adaptive beamforming techniques.

Short-duration wideband snapshots will be used to quantify the co-channel environment as a function of frequency. Long (~1 second) wideband snapshots will be tasked for LPI data collection. Additionally, the narrowband snapshot collect mode can be tasked at up to 1 MHz bandwidth, which is sufficient for many of the LPI tests and may therefore be used to reduce downlink times and/or to increase the collect duration to improve doppler resolution (nominally 2 sec at 1 MHz bandwidth, 6 antennas).

5.3.2 Ground Element Architecture

The Ground Element hardware consists of a Sun Sparc 5 workstation, running the Solaris operating system. The data link interface is assumed to be 10/100baseT ethernet compatible, and the interface between ground and air elements is assumed to be functionally equivalent to a small local-area network. All subsystem communications are performed through standard TCP-IP and FTP protocols.

A block diagram of the Ground Element functional components is given in Figure 5-5. The Ground Element hosts the overall system command and control HMI, through which the operator performs system setup and initialization, and controls the Air Element functions. The capability will be provided to task snapshot data collects, save them to files, and process them in batch mode with MatLab-based data analysis tools to validate the collects and/or quantify the collection co-channel environment in pseudo-real-time.

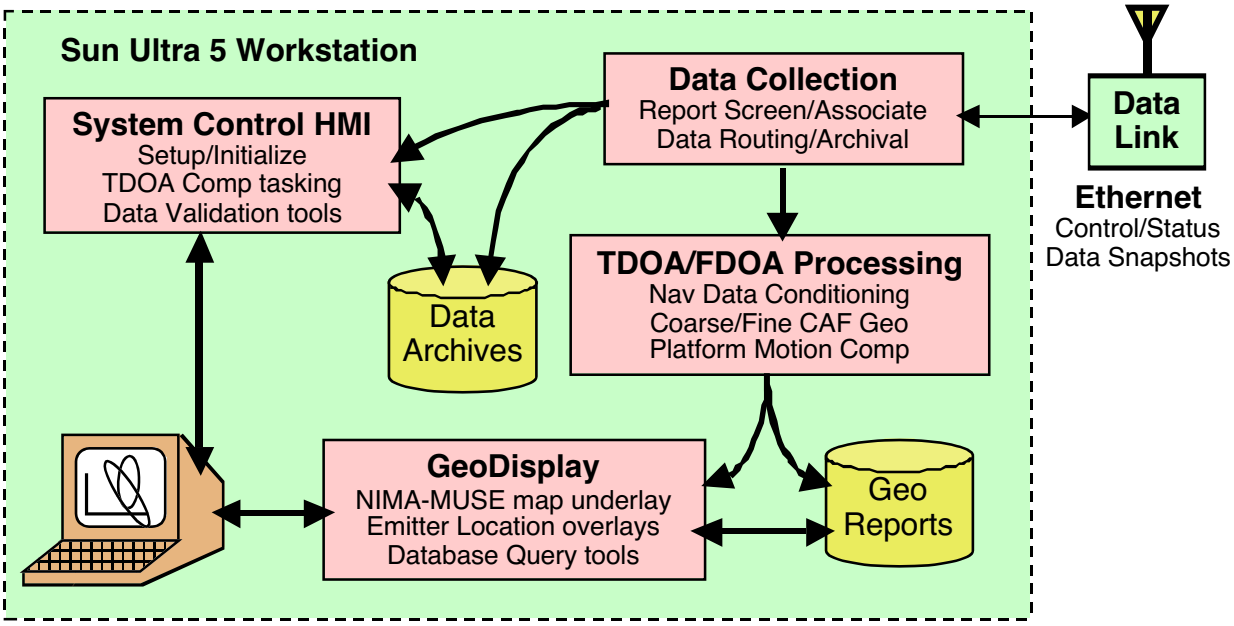

Figure 5-5. Phase 2 Flight Demonstration System, Ground Element Functional Diagram.

The Ground Element tasks TDOA compensation collects and processes the resulting snapshots to determine the compensation filter coefficients. These coefficients are then uploaded to the Air Elements to update the equalization filters. TDOA compensation may be performed either periodically or manually upon operator request, depending upon the receiver group-delay stability and accuracy requirements, both to be refined under contract. Currently we expect that the receivers are sufficiently stable, once warmed up, to require only infrequent TDOA compensation, perhaps even only once immediately after retuning to a new frequency channel of operation.

During normal PinPoint Demonstration operation, the beamformers on the Air Elements "push" signal detections and associated copy data to the Ground Element. The detections are screened based on collect duration (to screen out interfering LPI dwells) and associated based on signal-up timing. Associated pairs of collects are routed to the TDOA-FDOA processor along with navigation data over the duration of the collects.

The TDOA-FDOA processor conditions the navigation data (reformatting, coordinate conversion, filtering and resampling/interpolation), performs motion-compensated cross-ambiguity (CAF) processing and determines target latitude-longitude and estimated error ellipse

parameters. These parameters, along with time-of-detect, are passed out to the GeoDisplay program for databasing and display in real-time on a map.

The map display software used for Phase 2 flight testing (and beyond) can be the GeoDisplay application developed for the Phase 1 demonstration, which is discussed in detail in Section 4.1. An alternative option currently under consideration is the integration with the Government-supplied GALE-LITE ground station situational awareness software tool.

5.4 Phase 2 Flight Test Objectives

The flight test has three main objectives. The primary objective is the demonstration of precision geolocation of low-power conventional single-channel emitters in a dense co-channel interference environment, broadcast TV in particular. The second, but still high-priority objective, are to collect narrowband data for further refining the conventional geolocation algorithms to improve their sensitivity. The final objective is the collection of wideband data to refine and demonstrate LPI geolocation performance in Phase 2 post-test data analysis and/or early in Phase 3. The details of the flight test plan are to be defined in coordination with the Government, but the following sections are given as a notional concept of the flight test effort currently envisioned by Radix. The flight testing will be limited to the available Government supplied radios, flight track areas, number of flights, frequency authorizations, available emitter sites, and test emitter support staff.

5.4.1 Test Equipment and Preparation

Substantial Government support is required for a successful test, first and foremost with regard to flying the two Guardrail testbed aircraft, and providing the ground facility and data links. In addition, Radix currently plans on using Government-furnished conventional and LPI radios as the test emitters. Ideally, the Government would provide several multi-mode single-channel VHF radios that could operate anywhere in the 30-90 MHz band, with conventional AM/FM analog or FSK digital waveforms, as well as LPI with a number of selectable bandwidths, and with selectable transmit power levels. Radios operating at UHF, particularly LPI radios, would also be useful for validating the motion compensation approaches at the higher frequencies.

Radix expects the Government to supply the following to support the flight test program:

- Two (2) Guardrail aircraft with pilots, maintenance, support including:
  - Data link, ground facilities
- Coordination with FAA on use of flight track areas
- Conventional and LPI test emitters in both VHF and UHF bands
- Approved frequency authorization for use of GFE radios
- Emitter sites for the proposed testing. Sites should be surveyed to a location accuracy much greater than the accuracy expected of the system. Emitter sites need to support a wide variety of test scenarios. These test scenarios include: closely spaced nets, widely spaced nets, sites with diverse ranges to the flight track areas, sites in a variety of angular

orientations with respect to other sites and local broadcast TV (channels 2-6) signals. Some tests should be performed with emitters positioned near the towers and/or in positions that will be nearly colinear with towers from the perspective of the platforms over some portion of their flight path, in order to demonstrate the ability of the beamformer to copy the signal by nulling co-angle but horizontally polarized TV on the basis of polarization. Note that even with fixed emitter survey locations, the co-channel scenario can be changed completely by retuning to a frequency in another TV channel, or outside of the TV bands entirely.

- Staff to operate test emitters to a scripted plan. Each radio operator should also have a cellular telephone as an independent communication link for scenario coordination and scripting.

Post-flight analysis efforts planned in Phase 2 are primarily focused on quantifying the observed geolocation results, but also include using snapshot data collects to refine and demonstrate the geolocation algorithms for the case where only one platform detects the signal of interest. Snapshot collects of LPI radios will be used to refine and demonstrate the LPI geolocation techniques under the LPI development option. It is expected and desired that the flight tests will also yield a quantity of additional data to support future analysis and algorithm refinement efforts not funded under Phase 2.

5.4.2 Test Scenarios

Tests of conventional-signal geolocation should be executed with widely distributed nets operating at moderate power levels (e.g. 10 watts ERP) as well as closely spaced nets operating at low power (1 watt ERP or less), at various ranges and under varying levels of co-channel interference. Additional tests should be performed at clear frequencies as close as possible to the desired frequency of operation in order to quantify actual received SWNR levels for the emitters in each test geometry. It is desirable to create scenarios that test the target location accuracy at the limits of detectability, preferably through distance (possibly by enlisting the support of personnel at other facilities to save on travel time) but if necessary through reduction of transmit power.

Assuming the test radios support multiple modulation formats, tests should be performed using a variety of modulations. Demonstrations require the use of constant-modulus waveforms in order that the signals be stably acquired by the beamformer, e.g. FM-voice, FSK or PSK. Standard AM voice (double-sideband with unsuppressed carrier) is also stably acquired by the beamformer and may also be used as a secondary test waveform, but is not currently recommended for use as the primary test waveform

The scenarios should be scripted to provide various levels of signal-on-signal as well, from none (single SOI at a time, against TV interference) to multiple simultaneous radios. If LPI radios are available, then tests should also be performed with LPI-on-conventional, especially with a strong LPI radio(s) located near the platform(s).

During the flight test, the wideband data snapshot capability will be used along with Matlab processing functions to provide near-real-time displays of the co-channel environment through “eigen-PAN” spectral displays. These displays are generated by channelizing the snapshot data,

computing the covariance matrix in each channel, and computing and displaying the ordered eigenvalues of the covariance matrices as a function of frequency. These displays indicate the number of co-channel signals and relative strengths as a function of frequency, or equivalently, the interference floor obtained after steering respectively 0, 1, 2, etc. nulls. The information is needed to quantify the co-channel environment severity seen at each platform which is in turn needed to select good test frequencies of operation.

The primary gelocation testing will be performed with stationary emitters. As test time permits, some tests should be made with slowly moving emitters (e.g. the operator walking in a circle about the ground-truth survey point with a hand-held radio or transmitting from a moving vehicle) to quantify both geolocation bias errors and Doppler decoherence.

The primary geolocation tests will be made with the platforms flying on typical racetrack (straight-line) flight profiles. As test time permits, additional testing could be performed with nonstandard flight paths, for data collection in support of advanced beamformer phase stabilization and motion compensation efforts. Simple flight path possibilities might include short racetracks, figure-eights, or shallow "S" turns where the aircraft is slowly rolled from one side to the other along an otherwise straight flight path.

5.4.3 Data Collection

The raw navigation data from both platforms will be archived for the duration of all flights for future reference against other collected data, and possibly for post-flight analysis to refine the navigation smoothing and interpolation algorithms. This data can also be used for model development to improve the fidelity of future simulation efforts, and/or for direct incorporation into those simulations.

A typical geolocation test might proceed as follows. Once the test radios are in position, their transmissions are monitored on a clear frequency in order to quantify actual received SWNR, which is given by the beamformer signal-up detection statistics. The raw beamformer detection statistics can be archived and/or displayed and the data noted in a notebook. The scripted test is then performed at the desired frequency(ies) of operation (with TDOA compensation being performed at the start of each new frequency of operation), and locations archived for post-flight performance analysis against the scenario script. Multiple geolocation tests will be made at each test configuration to obtain a statistical characterization of the location performance.

The primary test frequency band is VHF with some tests performed beneath TVI. If UHF radios are available, tests should be performed at UHF frequencies as well, although since the approved frequencies of operation are generally outside of the UHF or High-VHF Broadcast TV bands, the radios themselves have to be used as interferers via signal-on-signal scenario scripts. Tests at UHF are of value primarily to test the navigation data processing and motion compensation algorithms at higher frequencies (shorter wavelengths).

Some number of narrowband snapshot collects (multi-antenna, both platforms) should be acquired for post-flight analysis of short (e.g. 30-90 sec) tightly scripted scenarios. These snapshots should be focused on "problem" cases where unexplained performance degradation is experienced and cases where some of the emitters are not detected at one or both platforms. As

time permits, snapshots of special test cases, including nonstandard flight paths and/or moving targets along with control collects with straight flight paths and stationary targets, and tests conducted at TV audio subcarrier frequencies, will be collected and archived for future analysis.

5.4.4 LPI Data Collection

Radix also strongly recommends the collection of wideband snapshots for LPI emitters in support of the parallel PinPoint LPI geolocation efforts. The Eclipse tuners support a one-second snapshot of full-bandwidth (15 MHz) raw A/D data, but downloading a six antenna snapshot on a 10-base-T ethernet link would take about 10-15 minutes, so full-bandwidth collects may be operationally expensive. In contrast, a two-second snapshot of a 1 MHz subband can be downloaded in 1-2 minutes, so where possible we will adjust the bandwidth of the LPI emitters to limit the required bandwidth of the LPI collects.

The scenario scripting for LPI collection is considerably simpler than for conventional signals. For LPI collection, the test emitters to be collected are required to be on for the duration of a 1-2 second snapshot, but do not require any further scripting or key-down synchronization.

A basic Matlab-based snapshot analysis capability will be used to compute and display the LPI co-channel detection statistic in order to validate the collect. This tool, or a similar tool, will also be used to quantify the LPI SWNR levels by processing snapshot data acquired in a clear band, e.g. below TV Channel 2.

LPI tests of interest include collection at various SWNR levels under various co-channel interference conditions and with various numbers of simultaneously emitting LPI radios. Data should also be taken at various LPI bandwidths to test performance with partial-band collects. Data should also be acquired for turning-platform and/or moving-emitter scenarios. Snapshots should also be collected at UHF for these cases, if UHF LPI radios are available, since any path-length errors will cause greater phase decoherence at the shorter wavelength.

5.5 Pinpoint Long-Term Migration Plan

The long-term plan for PinPoint is of course still highly flexible at this point in time, but an overall plan is nonetheless needed in order to properly steer the current and near-future effort.

5.5.1 PinPoint Phase 3

Pinpoint Phase 3 will expand the test system to process signals from LPI transmitters and will perform testing with both LPI and conventional transmitters. The LPI signal processing requires implementation of a wideband channelized co-channel detection/DF processor, DF array calibration, and a deep wideband buffer memory to support look-back filtering and beamforming in the airborne hardware. Migration from the Phase 2 airborne test systems will be achieved by adding G4 processors and software. The receivers and other RF equipment used for Phase 2 flight testing support the wide instantaneous bandwidth signal processing required for this phase.

The Phase 3 system will be architected as a staring asset under this program plan. Wideband scanning spectral search functions and extended-dwell drop-receiver support could also be

supported in Phase 3 as an option, or deferred to Phase 4 implementation at the Government's discretion.

5.5.2 Pinpoint Phase 4

Pinpoint Phase 4 will integrate Pinpoint into a host system that has the capability to perform full SIGINT signal processing. At this stage it is envisioned there are several possibilities for the host system architecture. One obvious choice is migration of Pinpoint to LBSS. The LBSS system architecture is designed to support peripheral functions required for Pinpoint such as data sample synchronization to within 20 nS for multiple channels and multiple payloads, and dynamic receiver group delay compensation using precision timed BPSK test signal injection into the RF front-end.

Other possibilities for a host system include the Division and/or Corps Tactical UAV SIGINT payloads and ACS. The current PinPoint architecture could also be evolved into a full co-channel SIGINT capability and inserted into the Guardrail platform as a front-end upgrade.

5.5.3 Final Comments

For the near-term PinPoint flight testing plans, the emitter geolocation processing will be performed on the ground primarily for testing convenience and expediency. Various platform and end user link modes are envisioned as candidates for ACS as shown in Figure 5-6. To support these modes, the emitter geolocation processing must eventually be hosted on-board the platforms to minimize system complexity and data link requirements.

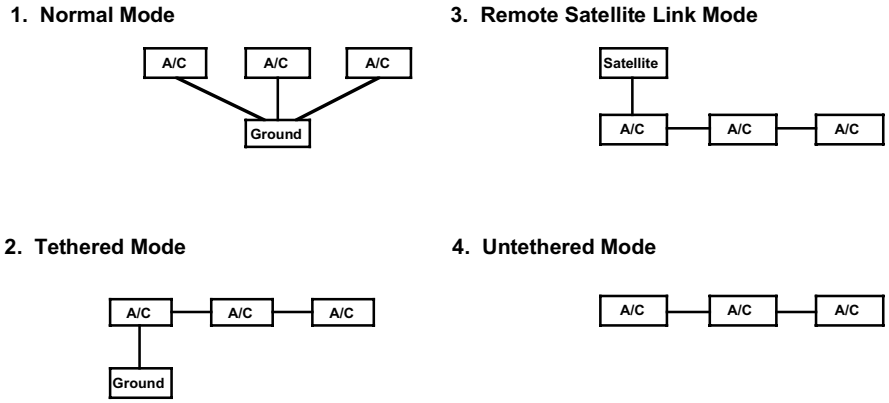

Figure 5-6. Candidate Multi-Platform Interlink Modes

The Pinpoint migration plan as presented here is intended to provide a launching-point for further discussion, and as a vehicle to solicit Government inputs regarding the PinPoint program, in order to better establish the scope and expectations of both the near-term and long-term Pinpoint development phases.

6. Conclusions and Recommendations

The PinPoint Phase 1 effort provides the Government with a useful simulation-based beamforming geolocation and display capability that can be readily integrated with the required data interfaces for actual flight-testing of the conventional tactical signal geolocation algorithms in Phase 2.

The GeoDisplay HMI provides a useful yet efficient display capability that supports projected PinPoint flight testing requirements through Phase 2 and beyond. Options to transition to Gale Lite or other more comprehensive ground-station software packages are being kept open, but the current capability is considered entirely adequate at this point for purposes of PinPoint demonstration.

Our HMI recommendation is to use the current display until such time as the Government finalizes its decision on the Tactical-COMINT support software to be employed by the Distributed Common Ground Station – Army (DCGS-A) architecture.

The LPI fine-CAF algorithm developed on Phase 0 was refined with the addition of motion compensation algorithms, and comprehensively tested in platform dynamic scenarios including turns and turbulence effects. The results are highly encouraging, and indicate that the motion compensation algorithms are both necessary and adequate, especially at UHF, and enable the coherent processing of sparse intercept data such as would be received from a full-band LPI emitter with partial-band staring assets. Intercept duty factors as low as 5-10% can be processed for precision geolocation with this approach.

The recommendation for LPI processing is to continue more detailed and comprehensive LPI implementation and simulation in MatLab under Phase 2. As a highly desirable option, we also recommend the acquisition of moderate-duration (several seconds), moderate-bandwidth (1-3 MHz) multi-platform multi-antenna I, Q data during the flight test with the test emitters operating in LPI mode, with post-flight MatLab processing in order to further validate the approach as programatically efficiently as possible.

The majority of the Phase 1 program effort was focused on the development of a conventional signal geolocation capability that is closer to a flight testable implementation than had originally been planned for Phase 1, in order to expedite flight testing of conventional geolocation during Phase 2. In return for deferring further development of the LPI algorithms, the conventional algorithm development tasks were upscoped to include:

- A self-contained conventional signal detection and beamforming module, implemented on a VME quad-G4 DSP card;
- Narrowband I, Q data simulation capability including conventional net traffic, TV and LPI interference, and changing platform dyanmics representative of collect times on the order of several minutes;

- Data interfaces and algorithm integration into an end-to-end system implementation, with a much more flight-test-like architecture than had been originally envisioned for Phase 1, but that addresses only conventional signal geolocation.

Detailed recommendations and plan revisions were made for the Phase 2 program and beyond, in support of an accelerated and incremental flight test schedule. Under the original program plan, flight testing was not scheduled until Phase 3, but was to include testing of LPI geolocation algorithms as well. Under the accelerated plan, conventional signal geolocation will be flight tested in Phase 2. The detailed algorithm implementation and simulation work for LPI geolocation will be performed also in Phase 2. If possible, LPI data collects should be acquired during the conventional signal geolocation demonstration flight tests and used to validate and refine the LPI algorithms with offline Matlab analysis. Implementation and flight testing of the LPI algorithms is deferred to Phase 3.

7. Military Significance

The PinPoint Multi-Phase Program, especially in conjunction with the Radix-Army NRC Multi-Phase Program, will comprise a major step toward providing the Government a complete co-channel interference mitigating search-detect-identify-geolocate SIGINT system implemented on a highly modular, scalable and reconfigurable COTS-based architecture. The comprehensive integration of co-channel interference look-through capability into the architecture enables the battlefield environment to be accurately monitored in real-time deep behind the forward troops, from airborne collection platforms such as Guardrail or ACS positioned at safe standoff distances.

The robust NRC classification algorithms offer an unprecedented level of performance compared to conventional approaches to signal classification. Accurate classification and parameter estimation is obtained at low SINR levels even when the background interference is dominated by a lower-level signal of another modulation type. When combined with beamforming detect-copy techniques, NRC yields highly accurate results down to the limits of signal detectability for all single-channel tactical modulations.

The co-channel interference mitigation techniques employed by PinPoint yield detection, DF and geolocation reliability and accuracy performance in dense co-channel environments that is similar to performance levels attained by conventional systems in clear (interference-free) bands. In addition, even in interference-free conditions, the co-channel beamformer approach provides coherent beamforming gain which enhances detection, classification and geolocation accuracy, especially for low-power short-duration signals. As a result, even modern, low-power single-channel tactical emitters operating in closely spaced nets underneath broadcast TV interference will be reliably detected, copied, classified and precisely geolocated at standoff ranges of 200-250 km.

PinPoint capabilities can also be integrated with LPI emitter association and tracking techniques to form a powerful solution to the HF SSB-Voice LPI problem. Large numbers of such emitters can be robustly resolved and tracked, and high geolocation accuracy can then be obtained on individual transmissions via coherent post-track integration.

This combination of technologies will yield a dramatic improvement in battlefield mapping capability beyond that of currently fielded systems. The system detection and copy footprint is greatly increased, enabling standoff coverage of the entire battlespace for even low-power handheld emitters with a high probability of intercept even in dense interference environments. As a result, accurate classification and precision geolocation is obtained on individual emissions for a comprehensive and real-time situational awareness and battlefield mapping capability, which in turn enables greatly enhanced emitter tracking and network analysis capabilities.

8. Glossary

ACS	Aerial Common Sensor
ADC	Analog to Digital Converter
AOA	Angle of Arrival
AOI	Area of Interest
BF	Beamform
CAF	Cross Ambiguity Function
CC	Co-channel
CEP	Circular Error Probability
CMA	Constant Modulus Array
CONV.	Conventional
CONV. Impl.	Conventional Implementation
CONV. Sim	Conventional Simulation
DD	Differential Doppler
DET	Detect
DF	Direction Find
DMP	Dominant Mode Prediction
FDOA-DD	Frequency Difference of Arrival – Differential Doppler
FEBA	Forward Edge of Battle Area
FIR	Finite Impulse Response
FLOT	Forward Line of Troops
FSC	First Syllable Copy
GDOP	Geometrical Dilution of Precision
GPS	Global Positioning System
HMI	Human Machine Interface
INS	Inertial Navigation System
KCSPS	Kilo-Complex Samples Per Second
KT	Knots
LBSS	Low Band Sub-System
LCMC	Low Capacity Multi-Channel
LOB	Line of Bearing
LPI	Low Probability of Intercept
MGN	Modified Gauss-Newton
MT	Multi-Target
NB	Narrow Band
NRC	Non-Linear Resonance Classifier

NSME	Normalized Mean Square Factor
ORD	Operational Requirements Document
OXCS	Master Oscillator (Oven Controlled Crystal Oscillator)
PRE-D	Pre-detection
RSSS	Rapid Spectral Spatial Scan
SAW	Surface Acoustic Wave
SOI	Signal of Interest
TDOA-DD	Time Difference of Arrival – Differential Doppler
TUAV	Tactical Unmanned Vehicle